



HAL
open science

Diamond biosensors

Clément Hébert, Sébastien Ruffinatto, Philippe Bergonzo

► **To cite this version:**

Clément Hébert, Sébastien Ruffinatto, Philippe Bergonzo. Diamond biosensors. Carbon for Sensing Devices, Springer International Publishing, pp.227-264, 2015, 9783319086484; 9783319086477. 10.1007/978-3-319-08648-4_9 . cea-01818477

HAL Id: cea-01818477

<https://cea.hal.science/cea-01818477>

Submitted on 17 Mar 2020

HAL is a multi-disciplinary open access archive for the deposit and dissemination of scientific research documents, whether they are published or not. The documents may come from teaching and research institutions in France or abroad, or from public or private research centers.

L'archive ouverte pluridisciplinaire **HAL**, est destinée au dépôt et à la diffusion de documents scientifiques de niveau recherche, publiés ou non, émanant des établissements d'enseignement et de recherche français ou étrangers, des laboratoires publics ou privés.

Chapter 9

Diamond Biosensors

Clément Hébert, Sébastien Ruffinatto and Philippe Bergonzo

C. Hébert · S. Ruffinatto · P. Bergonzo

Diamond Sensor Lab, CEA List, 91191 Gif-sur-Yvette, France e-mail:

Clement.HEBERT@cea.fr

Diamond is wide band gap semiconductor presenting many extreme properties. It is notably known as the most stable material with the highest chemical inertness, the highest mechanical hardness and the highest thermal conductivity [1–3]. Since the mid 1970s it has been possible to grow synthetic diamond by several methods. High Pressure High Temperature techniques that mimic the diamond formation in the earth's crust were first developed [4–6]. Then Chemical Vapour Deposition (CVD) methods enable diamond growth at laboratory scale [7–9] as well as the control the P-type and N-type doping of diamond [10–13]. Besides, it is possible to tune the diamond electrical properties from very resistive to metallic thanks to the P-type doping with boron [14]. Current achievements have enabled the development of diamond sensors that can operate in extreme conditions [15–17]. After being used for its mechanical and thermal properties, diamond was considered for chemical sensing. In fact the chemical stability and the close-to-metallic conductivity of diamond make it a powerful tool for electrochemical detection in various environment. Furthermore, the diamond is an ideal substrate for surface functionalization thanks to the wide and very known carbon based chemistry. Such a feature combined to the outstanding electrochemical properties of the diamond electrodes have enable the production of very efficient biosensors and biochips. Diamond is also an interesting sensor for medical imaging. Its carbon nature, well tolerated by living tissues, are actually very useful for its use as a biosensor capable of working in contact with bio-environments as well as real neuronal interfaces. Both those topics will be discussed in details in the following pages. In a first part an overview on electrochemical based biosensors and their performance is described. Then in a second half of the chapter, novel applications where diamond is directly used as an electrode for neural tissue interfacing is presented in details.

9.1 Diamond Properties and Novel Sensors

The outstanding physico-chemical properties of diamond can be exploited for the development of bioelectrical devices devoted to sensing or analysis. Diamond is an ideal substrate material for surface modification and sensitive layer achievement. Actually, many highly stable functionalization way inspired from carbon chemistry can be performed on diamond. Besides, the exceptional electrochemical properties of heavily boron doped diamond (BDD) set it up as a perfect electrode material for bioanalytical applications or design neuroprosthetics implants. Utilization of usual electrodes is prohibited in corrosive, acidic or basic media. The chemical inertness of diamond allows its utilization in every type of media. Furthermore, it shows an “anti-fouling” behaviour, this singularity ensure to diamond electrodes a good stability with no degradation of the electrochemical signal over time due to surface passive layer build-up [18]. Due to its sp^3 hybridization, diamond-like coatings have a natural inclination to be mostly biocompatible [19] towards living tissues [20–26]. Thus, the development of soft diamond’s MEAs gives rise to serious expectation for neural implant dedicated stimulation and/or monitoring [27].

On the other hand, the properties of hydrogenated diamond surface conductivity can be harnessed to develop SGFET (Solution Gate Field Effect Transistor). The mechanical properties are used for the development of MEMs. Networks of μ -lever whose functional ranges are equivalent to those of QCM (Quartz Crystal Microbalance) are devoted to detection in liquid media when surface acoustic wave sensors (SAW) are used for gas detection. Finally, many devices for the diagnosis and/or detection of molecules or target objects have been developed on the diamond. The latter can be a simple support associated to external detection methodology or a specific transduction tool. The various techniques for detecting and transducing reported in the literature for diamond-based devices are listed below with certain detection limit:

- Biochips devices mostly used fluorescence microscopy technique as revelation process. This technique allows the extrinsic and semi-quantitative detection of a few 10^{-15} mol l⁻¹ targeted species in solution. It shows a robust detection methodology used as reference measures in biomolecular recognition (DNA hybridization, antigen-antibody coupling...) [28].
- Electrochemical techniques based on the outstanding properties of heavily boron doped diamond. Due to the low background current and the wide electrochemical window of diamond in an aqueous medium, detection limits of the order of 10^{-12} mol l⁻¹ can be achieved [29]. In addition, electrochemistry allows the quantitative analysis of the detected redox species that is adsorbed/immobilized onto the diamond surface or present in solution.
- The field effect transistors (SGFET) developed onto diamond has a sensitive range in the same order of magnitude as the cyclic voltammetry technique. However its operating principle is based on the surface conductivity which does not allow a direct reading of the amount of species in solution without prior establishment, in defined measurement conditions (interaction time, temperature...), of a calibration curve. An important advantage of this methodology is the ability to detect species without any redox activity [30].
- At last, a set of MEMs/NEMs devices based on different physic-chemical properties of diamond. One finds diamond micro-cantilevers bring real opportunities in terms of transduction. The mechanical properties of diamond can allow their use in dynamic mode, resonant cantilevers, and in electrolytic environments. As for the SGFET the detection is mainly based on surface effects, detection limits closed to the electrochemical one can be expected while allowing monitoring of biological recognition phenomena in real time [31]. The outstanding properties of the diamond surface have led to Photonic Crystals development on polycrystalline diamond. Finally, surface acoustic wave sensors are the only type of diamond devices devoted to gas sensing. The huge sound speed propagation of diamond (72,000 km/h) is the main physical asset. Putting aside spectroscopic techniques, the main limit of every gas sensor is their lack of selectivity. Taking in

account that functionalization onto usual quartz SAW is quite prohibited; the attractive surface chemistry of diamond is a major advantage toward selective detection.

9.1.1 Electrochemical Detection

One of the major advantages of diamond for detection in complex media is its “anti-fouling” property. This latter enables to carry out many successive measurements without significant loss of sensitivity. Moreover electrochemical specific method devoted to surface regeneration has been developed [32], it ensures full ‘defouling’ and recovery of diamond electrode properties. For instance, BDD samples has been put in contact with media with high fouling potential as blood, wine, mud or crude during several months leading to a significant increase of capacitive current. The electrochemical regeneration process leads to a complete recovery of the electrochemical samples sensitivity.

9.1.1.1 Inorganic Compounds

Thanks to the large electrochemical window and low background current of in aqueous solutions, diamond electrodes can be used to detect very small amount of metals, lanthanides and inorganic species. Particularly nitrates, nitrites, nitrogen oxides and azides ions [33–36] or the sulfate ions [37] as well as silver and tin [38], cadmium, copper, lead and zinc [29] and mercury [39] can be detected in very low concentrations with diamond electrodes. In some cases [40], microelectrodes are used to further improve diamond electrodes detection limits.

9.1.1.2 Organic Compounds

Several teams reported low detection limit of unconventional organic substances thanks to diamond electrodes. For instance, the detection of pesticides [41], phenol derivatives [42], chlorine compounds [34], nitrogen bases [43], purines [44], polyamines [45] and TNT [46] were successfully carried out through voltammetry or pulses techniques. Compounds of biological interest like nicotine [47], neurotransmitter [48], hydrochlorothiazide [49] and in vivo dopamine [50] were also directly detected. Another approach deals with electrical impedance spectroscopy, Hamers et al. have detected specifically the E. coli K12 [51] on MEA. This not exhaustive list of examples illustrates perfectly the electroanalytical potential of diamond electrodes for direct electrochemical detection. Many other electrode material were used to detect these compounds but none of them can operate for long time because of the fouling process. Actually most of molecules mentioned above are likely to polymerize or react directly with the substrate because of their aromatic structure. The possibility to be regenerated quickly makes diamond a very efficient and reliable electrode for long term sensing [42].

9.1.1.3 Wastewater Treatment

One of the main water purification methods consists in the oxidation of organic substances through highly reactive radicals. There are different chemical pathways to generate such radicals in solution, the most famous being the Fenton process [52]. Diamond proved to be an efficient alternative method to such chemical processes. As previously discussed, diamond electrode can operate at very high anodic potentials thanks to its large potential window [53]. It is thus possible to generate highly reactive OH radical to degrade organic substances in the vicinity of the electrode. Then, electrochemical treatments of water polluted with biocides [54, 55], organic acids and EDTA [56],

herbicides [57] was successfully achieved on diamond electrode. Such electrochemical treatments were also considered for the degradation of inorganic compounds such as cyanide [58], sulfates [37] or nitrate [50]. Moreover, Furuta et al. [60] demonstrated legionellosis deactivation by electrochemical treatment on diamond. Rodrigo et al. [61] have also proceeded to the entire deactivation of municipal wastewater infected by E. Coli, they shown that no desired or hazardous buy-product appeared during the treatment. Thus, the treated water can be reused [62]. Such nice results led to the implementation of commercial diamond electrodes in the treatment process of drinking water and swimming pool. However some limitations need to be considered. First, the radicals are so reactive that a dismutation process quickly appears and generates hydrogen peroxide. Second, the amount of organic species that can be degraded by the electrode is limited by the diffusion process. Specific devices must be added (fluidic, stir) to concentrate the organic species at the surface of the electrode. Finally, in order to degrade organic waste the targeted compounds have to be soluble in water.

9.1.2 Biochips

Biosensors and biochips are advanced analytical devices made of one or several biological probes (DNA, enzymes, immunoglobulins superfamily, antibodies, proteins, peptides...) immobilized on a support/functional material. Variety of bio-receptor has been grafted onto diamond due to its versatile surface chemistry allowing classical carbon chemistry reaction and coupling. Moreover, diamond acts as an active transducer and its physico-chemical properties are used in order to turn the recognizing signal into an electrical one. The following paragraphs will draw up a list of different biochips and biosensors that were achieved on diamond.

The expansion of research themes in biotechnologies, medical diagnosis, food processing and environmental quality control has led to significant biochips development. The advantage of biochip remains in multiparametric studies based on molecular recognizing onto a single substrate. The devices readout can be carry out through electrochemical, micro-gravimetric, micromechanic or optic methods, fluorescence microscopy stand as the common detection technique. The information multiplexing on a single substrate needs micro-devices as well as the possibility to graft molecules on a very small targeted surface. However, very few functionalization techniques allowed the localization and the parallelization of sensitive active species. Usual technique involves several steps and often requires lithography process. Therefore, the biochip achievement is tricky and long and cannot be easily scale up to industry without simplification of the sensitive layer achievement. Nevertheless, a new functionalization way based on the direct and spontaneous grafting of amines onto hydrogenated diamond [63] appears as the preferred technique for the direct grafting of biological species.

9.1.2.1 DNA Biochips

Yang et al. [64] were the first to achieve a DNA biochip on diamond in 2002. Two different nucleotides strand were immobilized in a local way through millimetric spot. This biochip needed 3 distinct functionalization steps for each ODN strand. The first step is the immobilization of a spacer arm containing an alkene group through photochemical functionalization of alkenes onto hydrogenated diamond. The diamond is dipped into the grafting compound solution and there are both exposed to UV light at 233 nm during 12 h under nitrogen atmosphere, two other steps are needed in order to immobilize the final probe strand of DNA. The grafting characterization was carried out through fluorescence microscopy. The revelation process consisted in the hybridization of the probes strand and their complementary strand previously tagged with a fluorophore. This biochip showed a good selectivity as well as a good stability. On the other hand its multistep type and the long exposure time needed restrict the multiplexing and so the biological information bring

onto the diamond substrate.

Zhang et al. [65] achieved a biochip thanks to the diamond surface amination through UV exposure under ammoniac. Before proceeding to the DNA coupling, several lithography steps following by octafluoropentane plasma lead to a pattern of fluorinated area acting as a mask during the final step. This latter consists in a chemical coupling between the amines of the diamond surface, as micrometric stops, and the modified probes strand. As for the previous result, the grafting revelation has been carried out through the hybridization of the labelled complementary strand and characterized by fluorescence microscopy.

Electrochemical functionalization processes appeared as serious alternatives to the previous techniques to decrease the grafting time of the primary function. This method is fast and allows the localization of the grafting. Nebel et al. [66] developed a micro-structuration technique of diamond leading to micrometric size of interconnected HBDD conductive areas surrounded by intrinsic diamond. Unlike Micro-Electrode Arrays, the conductive areas are interconnected and have size around 15 μm . The grafting of diazonium through electrochemical reduction was carried out. Then, several successive steps of chemical coupling are necessary in order to immobilize in a collective way on all the electrodes the same ODN strand. Nebel's team also reported a direct detection of DNA with an electrochemical method. The detection is based on the use of ferrocyanide as a nernstien probe in solution. It compared the intensity of DPV responses before and after the DNA probe grafting and after hybridation of the target strand to confirm or not the presence of complementary strand in the media. The detection limit is 10 μM . This technique is significantly faster than the fluorescence microscopy. However no multiparametric studies can be carried out because all the electrodes are interconnected. One can note that the microstructuration and the dissociation of the electrodes could decrease the detection limit. The massive appearance of inkjet devices allows deposition of few micrometer size droplets onto a substrate. Henceforth, using this MEAs and inkjet techniques, one can consider multiparametric DNA detection through electrochemistry techniques.

9.1.2.2 Antibodies and Proteins Biochips

Despite a large literature on enzymes immobilization for biosensors achievement, only few examples of antibodies or integrins grafting have been reported. Coffinier et al. [67] have immobilized labelled FLAG peptides onto diamond. The first step is the surface amination of a hydrogenated diamond sample through plasma under ammoniac. The second step is a chemical coupling leading to the introduction of a semicarbazide moiety as terminal function. The FLAG peptide is then chemically coupled locally by drop casting. The grafting is characterized by fluorescence microscopy through the recognizing of the FLAG antibody tagged by a fluorophore. Here, the spot size is around 100 nm. The specificity of the recognizing has been shown through the concomitant immobilization of a HA peptide and a FLAG one.

Hamers et al. [68] immobilized the E. Coli K12 through alkenes grafting by photochemistry followed by a set of chemical step allowing the coupling of the antibody through one of its available amine moiety. The functionalization was characterized by FTIR and the analyse of the spectrum allows them to conclude that the secondary structure of the protein has been preserved during the grafting. Using a similar functionalization process, Hamers et al. [69] achieved an antibody biochip dedicated to selective capture of the pathogenic bacterium E. Coli O157:H7 using the grafting of the E. Coli (O157:H7) antibody on UNCD surface. They find out that efficiency of the E. Coli bacterium capture on UNCD biochip is the same as those find on immunoassay standard material (Glass). On the other hand the stability of the grafted antibody on UNCD over time is significantly extended compare to usual materials. Indeed, the sturdiness of functionalized layers on diamond is stronger than silica or gold ones. Moreover they show that diamond doesn't affect the antibody activity over time, giving to the biochip several days of lifetime [69].

9.1.3 Biosensors

Biosensors combine a physico-chemical transducer and biological specie; they are analytical tool dedicated to specific analyte detection. The transducer will quantify the interaction between the analyte and the active biological specie to provide an optical, piezoelectrical, mechanical or electrochemical signal.

9.1.3.1 Enzymatic Biosensors

We will focus on amperometric biosensors through the example of the well-known glucose oxidase. The enzyme immobilization can be carried out by different ways: directly through a spacer arm or it can be encapsulated in cationic polyelectrolytes films, like PDDA, due to the isoelectric point of the Gox. In most of the case, the mere presence of the analyte will not be sufficient to enhance the enzyme activity and will require the addition of a co-substrate. Several quantifications techniques of the enzyme activity and so the concentration of analyte, here the glucose, in solution becomes available. Each of this means lead to a different generation of biosensor. One can define three generations:

- The first generation of biosensors is based on the direct detection at the electrode of one of the products of the enzymatic reaction. In the case of the Glucose detection through the Gox, it is the hydrogen peroxide. However, the use of this type of biosensors in complex media is limited. The oxidation of the hydrogen peroxide requires the application of a potential far from the open circuit potential. It occurs around + 0,65 V vs ECS on a platinumium electrode. Yet in complex biological media, the blood as an instance, numerous products exhibit similar or even lower oxidation potential (uric acid, ascorbic acid, glutathione...) that can interfere through the appearance of a nonspecific current separated from the enzymatic catalyse.
- The second generation of biosensors allows the detection of the enzyme substrate thanks to a redox mediator in solution or immobilized closed to the sensitive layer. It acts as an electron carrier; it may connect the prosthetic centre of the enzyme with the electrode or exchange electrons with the product of the enzymatic reaction. A large range of mediator can be found, the ferrocene is widely used with oxidases enzymes. The use of a redox mediator allows a decrease of the oxidation potential applied. One can note that in the last two cases, the electronic transfer between the electrode and the enzyme takes place at least through one transitional electro-active specie.
- The third generation of biosensor is based on the direct electronic transfer between the prosthetic centre of the enzyme and the electrode. This generation has a major advantage; it doesn't need the natural co-factor of the enzyme, which can be submitted to severe variation of concentration in vivo. The second advantage lies in the direct connection of the enzyme, it allows sensor utilization without redox mediator. This latter could interfere and even damage the target in complex biological media. At least, the redox potential of numerous enzymes is closed to 0 V. Thanks to this negligible potential, one can avoid any interference problem encounter in every complex media. The only limitation of this generation of biosensor depends on the prosthetic centre position towards the electrode. Indeed, in the case of enzyme with a substantial size, the prosthetic group could be deeply buried into the protein complex. This redox centre is sometimes so far from the protein surface that the direct connection remains impossible.

Dealing with the Gox, its Flavin Adenine Dinucleotide (FAD) prosthetic centre is so deep into the protein that a direct electric connection with the electrode is prohibited. Carlisle et al. [70] have been the first to immobilize the Gox onto diamond. They used the electrochemical reduction of the diazonium salts as a primary grafted layer. Thus they have achieved a first generation of

amperometric biosensor detecting the product of the enzymatic degradation, namely the hydrogen peroxide. As for every amperometric biosensor, the biosensor characterization was carried out through chronoamperometry method. Like every enzymatic reaction, the evolution of the current density according to the analyte concentration follows a Michaelis-Menten kinetics:

$$v = (V_{\max} [S]) / (K_d + [S]).$$

One can see that when

$$K_d \gg [S] \text{ then } v \approx V_{\max} [S],$$

the generation rate of the product is proportional to the substrate concentration. It matches the dynamic range of the biosensor.

When

$$K_d \ll [S] \text{ then } v \approx V_{\max} ,$$

the saturation regime is reached. From the chronoamperogram previously obtained, the calibration curve can be plotted. The glucose biosensor of the Carlisle's team shows a linear range between 0.5 and 5 mM, the sensitivity is about 1.3 $\mu\text{A}/\text{mM}/\text{cm}^2$ and the detection limit is 100 μM . The low reactivity of BDD electrode toward hydrogen peroxide has to be pointed out. The application of high oxidation potential is needed, here + 1.1 V vs Ag/AgCl, it will necessarily involve interferences with the media but can also cause irreversible damages to the sensitive layer.

Villalba et al. [71] have achieved a glucose biosensor through the immobilization of the Gox in a PSS (Poly(4-Styrene Sulfonic acid) film onto a Nitrogen Doped Nanocrystalline diamond substrate NDD. The detection and calibration have been carried out according to the same strategy previously detailed. In that case the chronoamperometry has been realized around + 0.6 V vs Ag/AgCl. The dynamic range of the biosensor is 1 μM –8 mM, that is compatible with the detection of hyperglycemia in patient suffering from diabetes. The detection limit is about 50 nM and the sensitivity is around 30 $\text{nA}/\text{mM}/\text{cm}^2$. Contrary to Carlisle and associates' work, the anodic current measure doesn't come from an enzyme monolayer but from a thick film in which multilayers enzyme equivalent is encapsulated. It explains the significant decrease of the detection limit and so the increase of the linear range. Nevertheless the current density is proportional to the concentration of the degradation product (hydrogen peroxide) at the electrode surface. In this case the Gox is not only located close to the surface. Therefore the provision of hydrogen peroxide at the electrode is limited by the diffusion into the polymer layer. Moreover the isotropic nature of the diffusion implies a loss of an amount of product into the solution. These contributions involved a significant loss of the sensor sensitivity.

One can note that the anodic potential used by Villalba et al. is lower than the one used by Carlisle. Nevertheless, it remains too high for certain applications. Olivia et al. [72] have partially removed this limitation adding some platinum nanoparticles at the diamond electrode surface. The platinum catalyzes the hydrogen peroxide oxidation and the glucose can be detected around an anodic potential of +0.4 V. This lower potential provides a better selectivity to the sensor.

Garrido et al. are the only one to have achieved a third generation biosensor dedicated to hydrogen peroxide detection on diamond electrode. In one case [73], they immobilized a catalase through a spacer arm grafted by the photochemistry of alkenes. The direct electrochemical coupling between the prosthetic centre and the electrode has been characterized by cyclic voltammetry. The redox couples observed are related to the oxidation states $\text{Fe}^{3+}/\text{Fe}^{2+}$ characteristic of the hemic prosthetic groups of the enzyme. The sensor operating is based on the hydrogen peroxide decomposition through the catalase, this step produces oxygen close to the electrode. Oxygen is electrochemically

reduced at the electrode through the detection of a cathodic current. The reduction potential needed is -0.4 V and the detection limit is 300 nM. The dynamic range of this biosensor is between 1 and 150 mM and its sensitivity is around $70 \mu\text{A mm}^{-1} \text{M}^{-1}$.

In a second article, the same authors immobilized the Horse Radish Peroxidase (HRP) [74]. The prosthetic centre of this enzyme also contains a hemic group closed enough to the enzyme surface to be directly connected to the electrode. The biosensor was achieved according to the same process than the previously detailed. The characterization of the HRP immobilization was characterized out by cyclic voltammetry, a characteristic redox couple appears around $+0.15$ V vs Ag/AgCl. In this case hydrogen peroxide is directly decomposed by the peroxidase and the diamond electrode acts as a co-substrate. The cathodic potential used for the chrono-amperometry measurement is $+0.05$ V vs Ag/AgCl. The dynamic range of the biosensor is between 0.1 and 45 mM, the sensitivity is around $2 \mu\text{A/mM/cm}^2$. One can note that the cathodic potential applied for the detection is really low and particularly suitable for investigation in complex media. A similar biosensor has been achieved by the same team. The HRP have been immobilized through a different primary layer. The diamond has been oxidized first and a silanization used to graft the spacer arm. The dynamic range has been significantly reduced. It points out how critical is the diamond surface state as well as the functionalization technique in the electrochemical properties of the sensors.

9.1.3.2 Field Effect Transistors

Field effect transistors (FET) are transistor using an electric field in order to control the channel conductivity of a semiconductor material. Usually, the semiconductor channel is located between the two electrodes (source and drain) and covered with a thin insulating layer. The characteristic of the FET is given by I_{DS} according to V_{DS} curve ($I_{DS} = f(V_{DS})$). In parallel, the Gate-source tension V_{GS} will modulate the conductivity. Therefore, a modification of V_{GS} will change the $I_{DS} = f(V_{DS})$ characteristic. One finds a significant variety of FET, the well-known is the MOSFET (Metal Organic FET). The technology, initially developed on silicon has been adapted on diamond. The first Metal-Semiconductor (MSFET) on diamond appeared in 1996 [75] and the first Metal-Insulator-Semiconductor FET (MISFET) in 1998 [76]. The most interesting FET type on diamond is the Solution-Gate FET (SGFET). This latter has based on the singular surface property of the hydrogenated diamond. The negative electron affinity of the H-terminated diamond [77] induces redox reactions between diamond surface and adsorbates. It involves a shift of the valence band edge above the electrons Fermi level in diamond providing electron acceptor levels [78]. Thus a charge transfer between diamond and the adsorbates is enabled [79] and a subsurface holes accumulation appears [80]. One can note that concomitantly, the conduction band is placed above the vacuum level and electrons can be directly emitted into vacuum with negligible barriers [81]. In SGFET, the electrolyte is directly in contact with the hydrogenated diamond surface. A reference electrode is placed in the solution and acts as the gate. This new transistor type has been realized in 2001 by Kawarada et al. [82]. Partial oxidation of intrinsic hydrogenated diamond allowed the achievement of pH sensors through surface conductivity modulation. Partial hydroxylation of diamond surface gives rise to protonation ($-\text{OH}_2^+$) and deprotonation ($-\text{O}^-$) of hydroxyl moiety involving a linear modification of the channel surface conductivity toward the pH.

These pH sensors can be used as enzymatic biosensors, Enzymes Modified FET (EMFET). Kawarada's team achieved the first EMFET in 2004 [83]. In a first step they proceed to a partial surface amination then the Gox or the urease is immobilized through the amines surface moieties. Prior to the enzymes functionalization the remaining hydrogenated surface groups have been oxidized in order to introduce surface sensitivity towards the local pH variations. Then, glucose or urea is introduced in the solution and decomposed by the enzyme. These reactions involve local hydroniums or ammoniums ions by-product generation, concomitantly a modification of the surface functions appears ($-\text{OH}_2^+$, $-\text{O}^-$, $-\text{NH}_3^+$). These successive modifications will lead to local depletion of the subsurface charge that modifies the channel conductivity of the FET and the

drain-source current decrease in a linear way. Linear range of the glucose and the urea sensors has been established for substrate concentration between 0.1 and 10 mM and 1 μ M and 10 mM respectively. The sensitivity of these two biosensors is respectively 10 and 30 mV/decade. Garrido et al. [30] have realized EMFET dedicated to acetylcholine and penicillin thanks to acetylcholine esterase immobilized through different ways and different surface terminations. They have drawn up a full table giving the different sensitivity of the devices according to the functionalization way and the experimental factors. One finds different DNA sensors based on SGFET devices [84]. To be selective, a DNA strand acting as probe is previously immobilized on a partially oxidized surface. After the hybridization of the probe with the complementary strand, the charge variation and in a lesser extent the local pH modification caused by the phosphate groups of the DNA close to the surface substantially modify the sub-surface carriers density and so the channel conductivity. In this device, the crucial point is the distance between the DNA probes and the diamond surface. It has to be smaller than the Debye length to avoid counter-ions or electrolytes screening effect. The sensors achieved in these conditions show interesting detection thresholds in the order of magnitude of the picomolar and also allowed DNA mismatches real time measurement [85]. Based on the similar principle, Kawarada et al. [86] achieved a biosensor dedicated to HIV-1 tat protein. A RNA aptamer with a highly specific recognizing potential toward HIV-1 tat protein was functionalized on a partially aminated surface. Then the RNA aptamer derived second strand is added in the media. In the presence of the targeted protein a duplex structure will appear. A part of the RNA sequence will specifically bind the protein and another part will be hybridized with the RNA strand probe. In the end the protein will be stuck between the two strands. The HIV-1 tat protein is significantly positively charge at neutral pH. When immobilized at the surface it involves a mechanic similar to the inversion layer capacitance in MOSFET. This capacitive layer density is around 1–5 μ F cm^{-2} when the detection threshold is below 1 nM.

Diamond SGFET has a noteworthy sensitivity and numerous perspectives in term of potential applications in biochemical and biological fields. Nevertheless their design involves several steps of lithography and the detection mechanism, based on surface charge effect, excludes the detection in complex and/or highly acid or basic media.

9.1.3.3 Microelectromechanical Systems (MEMs)

Due to its remarkable mechanical properties, and namely a high Young's modulus (>1 TPa), diamond appears as a suitable material for MEMS and NEMS fabrication with high interests for (bio)-sensing applications [87]. In this part, attention will be paid mostly on resonant cantilevers and in a lesser extent on Photonic crystal and Surface Acoustic Waves (SAW). After having demonstrated that NanoCrystalline Diamond (NCD) can exhibit Young's modulus value close to that single crystal diamond, Bongrain et al. [88] have fabricated diamond resonant cantilever using localized nano-seeding as selective nucleation method. The novelty of this approach is that it enables large area processing for large wafer scale fabrication with no particular clean room requirements. Dynamic mode has been chosen since in this regime the cantilever exhibits the highest sensitivity due to the combined effects of both mass loading and surface elasticity variations. This combined with the high Young's modulus makes diamond MEMS more attractive than their silicon counterpart for the same applications. The frequency modes of such a resonant diamond cantilevers measuring from 0.4 to 2 mm in length were extended from 70 to 4 kHz. This enabled the possibility to use such resonant cantilevers in liquid media, i.e. where other cantilevers cannot be used due to the too strong attenuation observed due to damping.

From this observation Bongrain et al. [31] have investigated the possibility to detect the smallest species detection in a liquid medium, i.e. the sole protonation of an acid radical. The system was realized from the immobilization of an aminocaproic acid on the cantilever. By tuning the pH above and below the pKa of this acid (4.5), it came possible to probe frequency shifts above 100 Hz. Usually dedicated to mass effect loading measurements only, it appeared that the physical effect

leading to frequency changes could not be associated with the proton mass but with the change in charge of the COO⁻ to COOH termination. According to its mechanical characteristics, these kinds of devices could be suitable for the detection of biological compounds from its extreme sensitivity to charge variations. For example, DNA detection has been carried out through the direct grafting of a DNA probe on the cantilever [89]. To improve sensor sensitivity, the probe has to be immobilized as it could from the surface in order to maximize charge effects at the cantilever surface. Hybridization has been characterized through fluorescence microscopy when denaturation has been shown through a frequency shift of 75 Hz. More recently Manai et al. [90] also realized a biosensor based on microcantilever and dedicated to 2-isobutyl-3-methoxypyrazine (IBMP) and 2,4-Dinitrotoluene (DNT), an analog compound for explosive TNT, specific detection. The biosensor is achieved through Olfactive Binding Protein (OBP) immobilization onto such cantilevers. OBPs are small sturdy soluble proteins found in olfactory systems that are capable of binding several types of odorant molecules. The DNT has been detected in the μM concentration range. Used as a probe for specific recognizing in this study, natural function of OBP is the non-specific binding of small odorant molecules. Thus, this kind of devices is going to be used for non-specific biosensors achievement. Different types of OBP can be immobilized on a microcantilever array in order to detect and identify explosives or drugs for instance.

A parallel domain of innovative diamond based sensors is that of photonic crystals (PhC). From a technology transferred from silicon, photonic crystals consist of 1, 2 or 3D periodic nanostructuring of dielectric materials allowing light guiding in the device. Photonic crystals are highly sensitive to local changes in their environment, such as the refractive index, which affects the resonance wavelength and the quality factor of the resonator and thus confer a sensing capacity to it. Blin et al. [91] have recently achieved 2D photonic crystals cavities fabricated in diamond and showed that a simple modification of the diamond surface termination could be clearly evidenced. It shows the possibility to realize very sensitive (bio)sensors dedicated to specific and/or nonspecific detection of gas species as well as (bio)chemicals in solution. In current works, various gases vapours have been detected on diamond PhC exhibiting different surfaces states and different surface functionalization [In press]. Sensors responses are greatly modulated according to the surface termination. In parallel, biotin has been functionalized on diamond PhC and on-line avidin detection has been carried out with a good sensitivity and selectivity [In press].

A last type of diamond MEMS sensor taking advantage of diamond surface functionalization was reported by Scorsone et al. [92, 93] where they simply use nanodiamond (diamond nanoparticles with size below 10 nm), that are deposited on top of a Surface Acoustic Wave (SAW) sensor. This technology is now mature but relies less on the real property of diamond as a sensor than it does as a functionalization support. We would not consider here as an active diamond biosensor and would advise the reader to refer to these articles [94, 95] for deeper investigation.

9.1.4 Conclusion

The large electrochemical window and low background currents of diamond electrodes in water allow the detection of compounds at levels that conventional electrodes cannot reach. Inorganics, organics, metals and lanthanides can be detected at low concentration. The association of the natural anti-fouling property of diamond and its unique regeneration process allows the detection of compound that reacts with the electrode during the detection. Moreover, due to its chemical inertia diamond tolerate the extended exposure to aggressive media. The surface chemistry of diamond enables to fabricate highly stable and effective (bio)-functionalized devices. The development of fast, simple and low cost functionalization techniques [96] could offer interesting alternative to established assays like ELISA technique. Associate to the singular surface conductivity of hydrogenated diamond extremely sensitive FETs devices have also been achieved. Such material is an outstanding opportunity for applications in (bio)sensors, detectors, implants, water treatment and

medical diagnostic in the years ahead.

9.2 Diamond for Neural Interfacing

9.2.1 *Devices for Electrical Neural Interfacing.*

Brain computer interfacing has been under massive development since the mid 1980s. Starting with the development of external recording of the brain activity, it is now possible to stimulate as well as to record a broad range of neuronal tissues with high signal to noise (SNR) and from wide brain regions to single neurons [97–101]. This led to many breakthroughs especially for alleviating pathologies affecting functional and sensitive nerve degeneration issues. Three families can be notably cited. (i) The deep brain stimulation technique developed by Pr Benabid that is now used to alleviate the tremor induced by e.g. the Parkinson disease and that has been successfully performed on more than 40,000 patients in the world [102–104]. (ii) The possibility to control a robotic arm with mental thoughts as reported by Keefer [105], where a brain computer interface translates neural activity of the brain into signals controlling a machine. And (iii) the recent significant advances reported on spinal cord regeneration and based on both drugs and electrical stimulation to enable leg motion on a paraplegic rat [106, 107]. These outstanding results were made possible partially thanks to use of micron size biocompatible electrodes, inspired from the technologies developed for silicon microchips. They opened the way to high spatial resolution and efficient communication with neural networks. The reduction of the size of the interfacial electrodes required for thin film deposition and stability that led to new materials and technical challenges. In brief, it is tremendously difficult to identify the type of microelectrode interfaces that enables to keep a high signal to noise ratio as well as a good charge injection. Many advanced electrode materials such as porous platinum [108, 109], carbon nanotubes (CNTs) [110, 111], more recently PEDOT [112, 113] or also iridium oxide [114, 115] were thus progressively developed to meet these requirements.

Nevertheless, when such microelectrode systems have come to real in-vitro or in-vitro experimental prototyping, several issues have progressively been identified to which biologists require material scientists to provide them with solutions. One of the main challenges for electrical neural interfacing is to develop highly stable and bio-inert electrodes for long term in-vivo studies. In fact the detection of a foreign body triggers an inflammatory reaction. This immune response leads to the formation of a protective cell layer that prevents the communication between the neural network and the electrodes [116–118].

Although the electrode materials mentioned above allowed keeping high SNR and high charge injection, they appear not to be sufficiently stable and reliable for chronic implantation [119–122]. Many approaches are under investigations to overcome these issues. For example, one consists of surface functionalization of the electrode or of the whole device, with drugs or proteins that prevent the inflammatory reactions. They are well summarized by S Chen and M. G. Allen [123]. Others consist in finding new materials, totally bio-inert that do not trigger any inflammatory reaction.

For this particular need, carbon and carbonaceous materials are remarkably good candidate to meet these demands. Their carbon nature is similar that of the body. SiC has been introduced in the previous chapters as a very interesting material. Carbon nanotubes were also thought to be very promising. Many studies were investigated demonstrating outstanding neural growth or very high signal to noise ratio with CNT coated electrodes [105, 110, 111, 124]. However the CNT application for electrical neural interfacing were precluded because of cytotoxicity issues due to their high aspect ratio geometry [125].

Diamond is certainly another good candidate. It is known to be chemically inert; it cannot be oxidized nor reduced by any materials or solutions. These unique properties led many teams to assess and prove the compatibility of diamond for the study of the living. More recently we proved

that retinal ganglion cells could grow on diamond without adding any protein coating. This is one of the rare materials for which it is possible. Above all it is the only conductive material available today that presents such an important property. Firstly used as biosensors because of their outstanding electrochemical properties (see previous section), diamond microelectrodes are now considered for direct recording or stimulation of the neurons. The aim of this section is to give an overview of the current diamond technologies developed for neural interfacing with a limit to electrical and electrochemical sensing with a strong emphasis on the electrical part. Further, new potentialities as provided by the exceptional features of the NV-centre for neural recording is not considered here but the reader is invited to have a look to this promising novel approach [126]. Below, in a first part the basic concept of neural communication are introduced to define properly the required properties of a material electrode. Then the diamond technologies are described and followed by some example of their applications. Finally some of the most advanced diamond electrodes are described.

9.2.2 *Communicating with Neurons*

The process at the origin of a physical, chemical or biological interaction must be rather apprehended in order to optimise a functional material that could sense this phenomenon. Hence, the communications inside the neuronal networks and its environment should be understood to determine the required properties of an electrode material that could be used for neural interfacing. The mechanism of the stimulation and electrical recording between the neuronal tissue and an electrode has been studied for long but the exact processes are still under investigations [127, 128].

The communication within neural systems is conveyed by two ways. The first one is the release of neurotransmitters. This chemical path is exclusively present between different neurons. The second way of communication is an electrical signal so-called action potential that propagates along a single neuron or from one neuron to another. The propagation of the electrical signal is due to a wave of depolarisation of the neuron membrane resulting from local ionic concentration changes.

According to the Goldman-Hodgkin-Katz equation [129, 130], increasing or decreasing the local ionic concentration at the neuron surface respectively increases or decreases the local potential and depolarizes the neuron membrane. Therefore, an action potential can be triggered if this depolarisation is sufficiently high. Likewise, an action potential induces a local change in the ionic concentration and thus a local variation of the potential at the surface of the electrode that can be sensed by the electrode. The ability to attract ions at the surface of the electrode can be evaluated by studying the capacitance at the electrode surface, so-called the electrical double layer capacitance [131, 132]. The higher the double layer capacitance, the higher the variation of ionic concentration at the electrode surface. The double layer capacitance can be determined by deducing the capacitive current obtained by cyclic voltammetry for several scan rates. The slope of the curve of the capacitive current versus the scan rate gives the values of the double layer capacitance.

$$C = \frac{\Delta i}{2v}$$

where Δi is the difference between the anodic and cathodic currents at a potential where no faradic current is recorded and v is the scan rate. The double layer capacitance can also be deduced from electrochemical impedance spectroscopy (see the impedance section).

9.2.3 *Basic Electrochemical Characterizations for Neural Interfacing*

We define here the appropriate electrochemical characterizations of an electrode to get the most relevant electrochemical properties for neural interfacing.

92.3.1 Cyclic Voltammetry

Cyclic voltammetry consists of recording the current yielded during a cyclic scan of the electric potential of the electrode. It is a useful characterization technique to determine the potential window of an electrode in a biological electrolyte and to get its double layer capacitance and the charge injection limit [133]. The charge injection limit is the maximum amount of charge that can be localized at the electrode surface without reaching the redox potential of the electrolyte. The charge injection limit can be in a first approximation determined by integrating the capacitive current on the whole potential window. Such a method is not completely accurate since it depends directly on the scan rate of the cyclic voltammetry. The frequency range is far below that of the actual pulses used for stimulation

92.3.2 Pulsed Techniques

Pulsed techniques such as fast chronoamperometry or fast chronopotentiometry consist of applying a current pulse or a voltage pulse of a few microseconds on the working electrode. It is this way possible to mimic action potential using biphasic pulses. These techniques are more accurate to determine the charge injection limit [133].

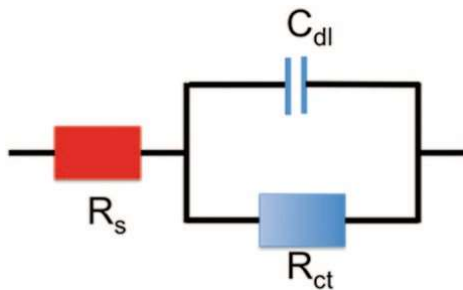


Fig. 9.1 Equivalent circuit of the electrode electrolyte interface

92.3.3 Fast Scan Cyclic Voltammetry

Fast scan cyclic voltammetry is a cyclic voltammetry technique used to get a high temporal resolution of the redox reaction. This technique is particularly interesting for the detection of quick phenomena such as the release of neurotransmitters [134].

92.3.4 Electrochemical Impedance Spectroscopy

Electrochemical impedance spectroscopy (EIS) consists of evaluating the ratio between the electrode potential and the current delivered by the electrode at different frequencies. It is a powerful tool to determine the equivalent circuit of the electrode to a medium interface. The possible charge exchange between a solution and an electrode can be either a direct electron exchange (faradic transfer) or a change of ion concentration at the electrode surface via a capacitive coupling. The most simple electrode-interface equivalent circuit is thus composed of a resistance (charge transfer resistance R_{ct}) in parallel with a capacitance (double layer capacitance C_{dl}) in series with a resistance (electrolyte resistance R_s) as described in Fig. 9.1. It is called the Randles circuit.

Most commonly, EIS is performed at a redox potential to evaluate the charge transfer resistance and the capacitive double layer for a given redox species. In the case of a neural interface, the EIS is

made in a physiological-like electrolyte like PBS at the equilibrium potential of the electrodes versus the reference electrode. EIS performed in an electrolyte containing redox species can also be considered provided the experiment is performed far from the redox potential of the reactive species. The charge transfer is very high in the case of EIS in PBS since no electron can be exchanged between the electrode and the solution. Thus, the electrode impedance is mainly driven by the surface capacitance.

The interfacial impedance has a strong influence on the thermal noise given by the equation [135]:

$$V_{th} = \sqrt{4 k_B T R_e(Z) B}$$

where k_B is the Boltzmann constant, T is the temperature, $Re(Z)$ is the real part the impedance and B the bandwidth of the electrode. The signal to noise ratio of an electrode for the recording of a neural signal should be as high as possible to get an accurate measurement. The interfacial impedance is also linked to the consumption power given by $P=ZI^2$.

The interfacial impedance of a microelectrode is far higher than that of a macroelectrode. This is due to the fact that the interfacial impedance increases when the electrode surface is reduced. We saw in the previous section that the interface impedance of an electrode can be basically modelled by a resistive element in parallel with a capacitor. The dependency relations that link the capacitance with the resistive element to the electrode surface are the following one:

$$C_{dl} = \frac{\epsilon_0 \epsilon_r S}{e} \quad \text{and} \quad R = \frac{\rho l}{S}$$

Where S is the surface of the electrode, e the thickness of the double layer, l the thickness of the electrode, ϵ_0 the vacuum permittivity, ϵ_r the equivalent permittivity of the double layer and ρ the resistivity of the electrode material. Therefore the double layer capacitance impedance and the charge transfer resistance are increased by a factor 106 compared to a 1 cm² electrode when the surface decreases down to a few tens of microns. This high impedance is one of the main drawbacks of the microelectrode for both stimulating and recording. High impedance, and consequently low SNR, can turn an electrode useless for neural recording. Likewise if the impedance is too large, the lifetime of the battery is reduced [136]. This is a common issue when implanted devices are always trying to reduce energy budgets. The issue linked to high impedance for neural recording can be partially solved by using a recording set up where the entry impedance is adapted to the interfacial impedance of the electrode [137].

9.2.4 *General Requirements for Microelectrodes Materials and Devices for Neural Interfacing*

9241 **Electrode Material Requirement**

Electrodes to be used for neural interfacing must comply with several requirements that can be associated with material properties. They can be divided in two categories: (i) basic properties, i.e. those required for an electrode material to be used in contact of living tissues for in-vitro and acute in-vivo studies and (ii) more advanced properties required for long term reliable neural prostheses. Both requirements apply for both stimulation and recording electrodes systems.

Electrodes require to exhibit (i) no cytotoxicity, as a primary features, or also referred to as high biocompatibility. Nor should interfacing devices result in cytotoxicity or into the modification of

the biological medium by inducing any chemical reaction and particularly during stimulation. (ii) Large charge injection limit: the material should exhibit a sufficient charge injection limit to trigger action potentials in the neural network. (iii) Low impedance: the impedance of the electrode should be low enough to yield high signal to noise ratio and allow low energy budget.

Further, material specifications must also provide (iv) high chemical and mechanical stability: the electrode material should be able to resist to the assaults of the body tissues in order not to be degraded. For instance metallic electrodes can be degraded by corrosion over time, particularly when the electrode is used for stimulation. Further more, the material should not be easily removed away from the device to ensure long reliability and avoid toxicity issues of dispersed material. In parallel, (v) biointeractions effects are a supplementary condition: the ideal electrode material should be invisible from the immune system. The detection of the material as a foreign body by the immune system triggers inflammatory reaction. In the case of neural interfacing, this would result in the coating of the implant by a thick layer of glial cells to insulate it from the neural network. This induces, at best a decrease of stimulation or recording efficiency, up to a complete loss of communication between the excitable cells and the electrodes with the consequence of rendering the implanted device useless. (vi) At last, since neuron interfacing is often aiming at probing degraded tissues, it is a real benefit if the stimulating material remains compatible with imaging techniques such as magnetic resonance imaging (MRI): MRI is one of the most efficient imaging technique for in vivo imaging of cell activity. The ideal electrode is thus transparent to magnetic fields in order not to alter in-vivo observations of the tissues in the near vicinity of the electrodes. This is a real challenge but it would also enable the study of the impact of in-vivo stimulation in the case of functional MRI.

9.2.4.2 Device

Similarly to that of the electrode material, the design of a neural interfacing device itself has to be optimized. While devices for in vitro studies are not very demanding in term of material engineering, those for in vivo studies require the development of very advanced technologies.

To start with, for in-vitro electrophysiology studies, the geometries of both the device and the electrode should be optimised in order to localise the electrodes as close contact as possible to the living tissues. This distance between the electrodes and the cells exhibits very significant impact on the SNR as well as on the possibility to trigger action potentials. Then, when implantation in the body becomes a condition, in vivo studies require further require the device to be flexible. This property offers the possibility for the device to be conformable to the implantation environment and then to put the electrode as near as possible to the living tissues. A flexible device is consequently less invasive and thus less aggressive toward the neural network it interacts with. Also, and as mentioned before, the ideal device should exhibit the least absorption to magnetic fields. If so, the material and the geometry of the device should not act as an antenna. The main current drawbacks of implanted devices as regard to MRI studies is the metallic wires that connect the battery to the device. They actually could interact with the magnetic field and induce local heating because of Foucault currents.

9.2.5 *Diamond Biocompatibility*

Biocompatibility is certainly the most important and difficult property to achieve from a material. Many materials have been reported as “non- cytotoxic”, however long-term use of electrodes or devices is often not possible because of degradation and rejection over the time. This is a particular issue for active and non-active implanted devices. Orthopaedic as well as neural, cardiac and other interfacing implants should not only be not-cytotoxic but also should be like transparent for the

body to avoid any inflammatory reaction and rejection.

The intrinsic chemical inertia of diamond was initially supposed to be a good indication of its biocompatibility. In fact, diamond cannot be degraded which is favourable for cell viability. The compatibility of any diamond forms, in term of cytotoxicity effect, has now been assessed for long with many kinds of cells. Several studies have investigated the influence of the diamond roughness, the diamond surface termination and protein coatings. All those properties were reported to have an impact on the cell growth. Also, since diamond electrode must be conductive, thus doped with e.g. Boron acceptor impurities, the influence of the boron presence in BDD was also considered to assess the biocompatibility of such diamond electrodes. Cell cultures were performed on diamond nanoparticles as well as in-vivo investigation of the ND cytotoxicity. They showed a high biocompatibility and they are very promising for cancer treatments [138–140].

Specht et al. proved that is possible to pattern neural growth (murine cortical neuron) on oxygen terminated single crystalline diamond by drawing a Laminine pattern with the micro-contact printing method [22]. The cells forms a network on the lines defined by the pattern. Moreover Ariano et al. showed the possibility of growing excitable cyliari ganglions on oxygen and hydrogen terminated single crystal diamond provided the substrates are coated with Poly-D-lisine or Laminine [21]. May et al. investigated the growth of rat cortical neurons on hydrogen and oxygen terminated boron doped nanocrystalline diamond (BNCD) [141]. Their study reveals no impact of the boron on the neural growth and a good biocompatibility of the two surface terminations with a better surviving rate for oxygen termination. The use of protein coating was compulsory for cells culture in all the studies above. However other papers showed that growth of cells could be performed even without any protein coating on NCD. Actually, Amaral et al. cultured MG63 and Humane Bone Marrow on as grown NCD for in vitro testing of bone regeneration [23]. The cells growth was promoted by NCD in comparison with the polymer control. This a good indication for use of NCD coating for orhopeadic implant coating. Bendali et al. recently reported outstanding properties of NCD for retinal ganglion cells (RGC) culture [142]. First a mixture of RGC and ganglion cells were culture on oxygen and hydrogen terminated on bare and PLL coated NCD. The glass control presented a higher surviving rate of RGC on the coated glass substrate than on the coated NCD but no difference can be seen when the substrates are not coated. However the glial surviving was better on coated substrates whereas the RGC survival rate was increased on non coated NCD. This indicates that NCD promotes RGC growth while preventing the development of glial cells. This would be helpful to prevent the encapsulation of diamond retinal implants.

9.2.6 Diamond Devices

The first application of diamond for electrochemical and biosensing consisted in coating materials to take advantage of the diamond biocompatibility and of its electrochemical properties [50, 143–145]. During the last decade, diamond and mainly nanocrystalline diamond cleanroom processing benefited from the same progress as that of silicon. Actually, most of the photolithographic processes can be applied on diamond as well as many plasma etching. It is thus possible to design diamond patterns. This advanced manufacturing opened the way for the development of diamond micro and nanosensors for a wide range of application. Rigid diamond microelectrode arrays showed the properties of the diamond combined to that of microelectrodes. They were first used for electrochemical sensing [146–151] and were more recently suggested and tested for neural interfacing [152–157]. Moreover, despite the high growth temperature of diamond some teams managed to transfer BNCD electrodes on polymer substrates in order to create flexible devices [158, 159].

92.61 Diamond Coating on Metallic Needles

The first diamond technology for in-vitro and in vivo interfacing was accomplished by coating metallic needle with BNCD. It consisted in seeding a metallic needle with diamond nanoparticles and to have them grown and coalesced to form a thin hermetic and biocompatible film at the surface of the needle. Figure 9.2 gives an SEM image of such a needle fabricated by Arumugam et al. [50]. This technology is very straightforward and proved to provide, even recently again [50], good electrode performances for neurotransmitter sensing. It can also offer a multiple site sensing or stimulation. However high spatial resolution cannot easily be achieved with this technique.

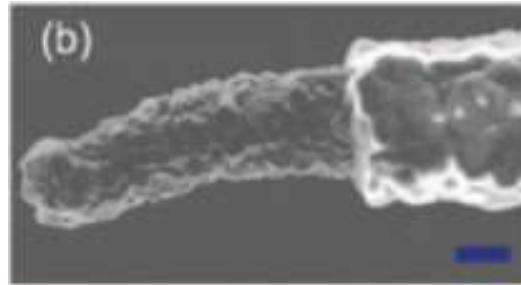


Fig. 9.2 Diamond coated metallic wire by Arumugam et al. [50] (used in accordance with the Creative Commons Attribution 3.0 Unported License). Scale bar: 10 μm

92.62 Diamond Rigid Addressable Classical Planar MEA

92.62.1 Boron Doped Diamond Addressable Microelectrodes for in vitro

Diamond addressable MEA were developed to record or to stimulate on multiple sites with a high spatial resolution. The MEA developed by Kiran et al. [154] from a collaboration between CEALIST and ESIEE-Paris is given to illustrate the micro-fabrication process of such devices. First diamond nanoparticles are fixed over a 4 in quartz wafer using a protocol described elsewhere [160]. Then an aluminium hard mask consisting of a disc of 100 μm in diameter was selectively deposited, over the areas where the BDD micro-electrodes have to be grown. Photolithography enabled to partially pattern the Al mask thus used to protect areas where diamond nanoparticles were protected from being etched in a reactive ion etching (RIE) process in oxygen. The Al hard mask was finally removed and the diamond electrode was grown. The dimensions of the resulting diamond disc electrodes were typically of 300 nm in thickness and 100 μm in diameter. Then an assembly of Ti (50 nm)/Pt (150 nm) metal tracks was deposited over the substrate with a metal ring going around the edge of the diamond disc in order to take electrical contact from the diamond electrode. Then a silicon nitride (Si_3N_4) passivation layer was deposited by CVD over the substrate. Finally an opening can be made over the diamond electrodes by using local etching of the Si_3N_4 layer by RIE with SF_6 gas. Typical dimensions range between 10–100 μm (Figs. 9.3 and 9.4).

92.62.2 All Diamond Arrays

The objective of this type of microelectrode array is to get an all carbon sensor. The active and insulating parts are made with boron doped and intrinsic diamond respectively. A process developed at the Neel Institute is provided as an example [155]. First a first layer of insulating diamond is grown on an insulating substrate. A BNCD layer is deposited on top. This layer is etched to reveal the electrodes, the tracks and the connection pads. Then the electrode and the connection pad are covered with a SiO_2 -Cr sacrificial layer in order to protect them during the growth of the insulating diamond layer used for the passivation of the array. The selective growth of

the passivation array prevents from any thickness inhomogeneity issues coming from the first two diamond layers or coming from the etching. The use of BNCD as conductive tracks is not straightforward since its conductivity is not as good as metals. Nevertheless they exhibited a series resistance of 4 k Ω . This value is far below the impedance of any electrode-neuron interface and would not introduce much more noise. A similar technology was developed by Chan et al. [152]. The only difference is the passivation process. Contrary to the previous technology, the whole conductive parts are first coated with an insulating diamond layer, then the contact pads and the electrodes are revealed by a dry etching. Moreover, the device is released from the silicon substrate at the end of the process. This technology also proved a very nice flexibility of the all diamond device (Fig. 9.5).

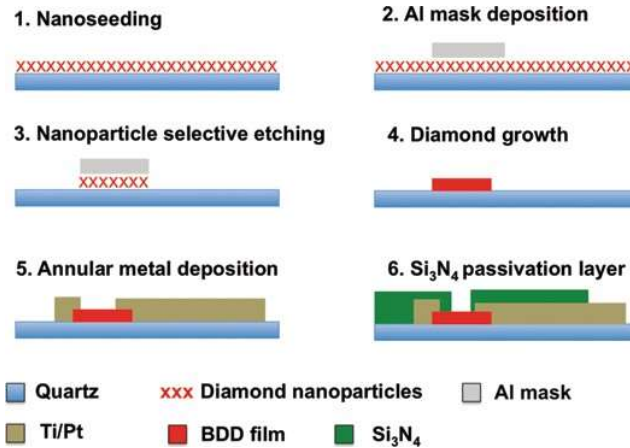


Fig. 9.3 Process for planar electrodes form Kiran et al. [154]

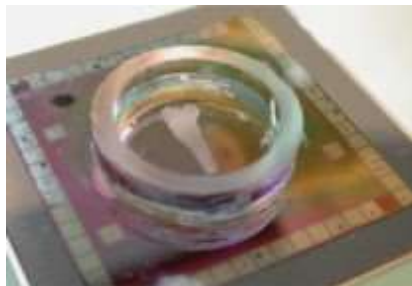


Fig. 9.4 Diamond MEA prototype for organo-typic measurements (CEA-ESIEE- INSERM)

9.2.6.2.3 Laser Printed Electrodes

Thanks to its carbon structure, it is possible to draw patterns on the diamond surface using laser lithography (direct writing). This technique was particularly used by Ganesan et al. [157] to build a planar all diamond microelectrode array. It consists of burning locally the diamond. This is a powerful tool to quickly and very efficiently draw a pattern during the optimisation phase of a design since it gives more freedom than that using rigid masks. Thanks to this microfabrication process, it possible to adapt quickly the device design to the tissues requirements (Fig. 9.6).

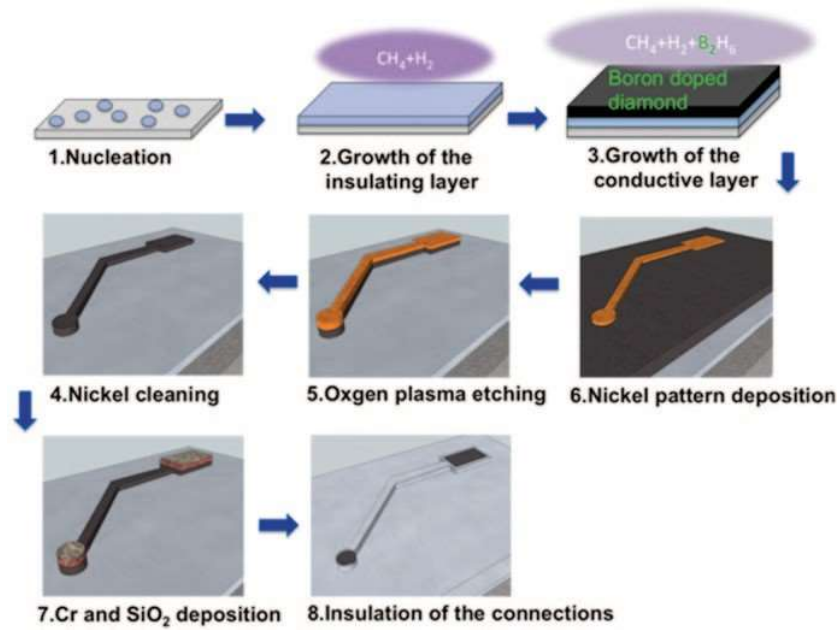


Fig. 9.5 An all diamond microelectrode array for in vitro studies from Hebert et al. [155]

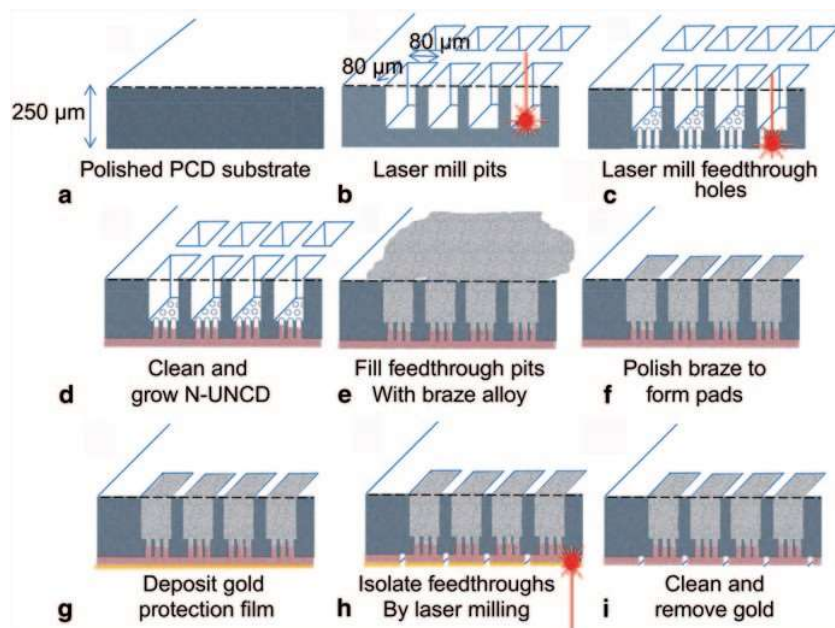


Fig. 9.6 All diamond (N-UNCD) microelectrode array from Ganesan et al. [157]

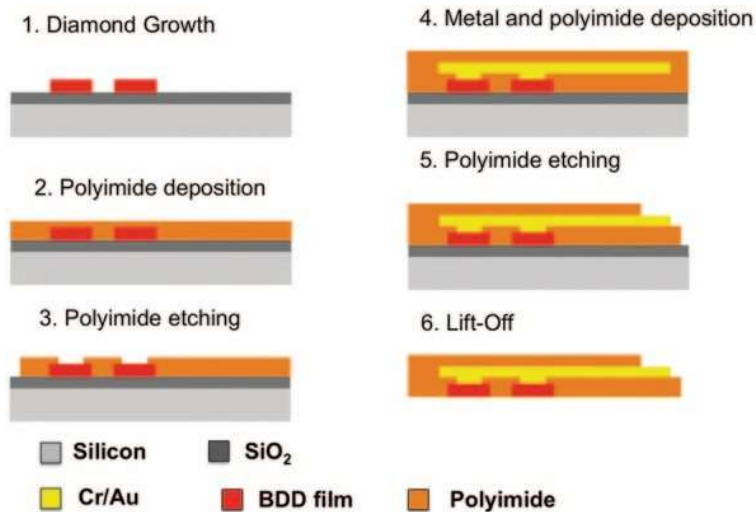


Fig. 9.7 Diamond flexible arrays for in vivo measurement from Bergonzo et al. [159]

9.2.6.3 Flexible Neural Probes

Flexible technology is a key point for the development of implantable electrodes. It actually reduces tissue-damaging when compared with rigid electrodes, and it allows a more conformal interface on the neural tissues [161]. The electrode can further be placed in contact with the neuron to enhance the efficiency of both recording and stimulation. The main constraint when in-vivo tissue stimulation is concerned is that the microelectrode array must conform to the size and shape of the tissues to be stimulated. This requires specific developments to enable the fabrication of devices that further to provide the advantages of the former ones must also be flexible and exhibit a long connecting foil enabling the electrical signals to be taken from outside the body to the in-vivo neuronal tissues. Despite the high growth temperature of the diamond Bergonzo et al. as well as Hess et al. managed to fabricate flexible implants with diamond electrodes thanks to a flip chip process approach.

9.2.6.3.1 Flexible Diamond Electrodes

The diamond electrodes are grown on a sacrificial layer. Then electrodes are embedded in a flexible insulating polymer. The polymer should be chosen carefully: it should not soak in water and should not degrade. Bergonzo et al. [158] suggested polyimide, which has been used for long as a polymer for flexible neural implants. Hess et al. suggested PNB [159]. The polymer was etched to access the electrode and connect them individually thanks to metallic track deposited by sputtering. The whole device was then embedded in another polyimide layer and release from the substrate thanks to a dry etching (Fig. 9.7).

9.2.6.3.2 3D Flexible Diamond Electrodes

The past decade has seen an explosion of research efforts into retinal prostheses aiming at restoring sight to patients blinded by retinitis pigmentosa or age-related macular degeneration. In addition to classical approaches, novel technologies are being explored, often in the context of newly founded commercial enterprises. Also, for the devices that will be offering a real breakthrough to blind people, theoretical studies have demonstrated that the ability to reach stimulation structures of 600 pixels would be of great benefit as it should be sufficient for patients to read [162]. A study driven

by the Vision Institute in Paris further rendered the specifications more challenging, as Djilas et al. demonstrated a very high interest in fabricating 3D wells where a small group of retinal [163].

Hence to meet this demand 3D diamond wells were developed [156]. The 3-D fabrication process is very challenging especially during the photolithography steps because of the high topography due to the surface mould. Therefore, the transferred patterns to a polymer (such as the electrode opening size) as well as metal layers patterning can be affected. For all 3-D processes, a thick photoresist is used to overcome these truncated cone structures without tearing at the topography edges. The process is then the same as described before.

9.2.7 BNCD MEA Electrochemical Performances

The electrochemical properties of the diamond microelectrode arrays were evaluated on diamond-coated needle and on microelectrode array. We only focus here on the electrochemical properties of the diamond electrodes in electrolytes without any reactive species.

9.2.7.1 Double Layer Charge Capacitance

The double layer capacitance of the microelectrode for neural interfacing has to be evaluated first in physiological like medium or in salt medium containing no redox species. All the reported articles showed diamond microelectrode exhibiting potential windows between 2.2 and 3.2 V in salt medium [143–157]. This indicates that no electrochemical reaction is initiated in a wide potential range if there is no redox species in the electrolyte. This confirms that the diamond electrode can operate safely at higher potential than any other material. Kiran et al. also reported some good statistics on a 64, 14 μm diameter microelectrode array in LiClO_4 , a medium pretty similar to PBS.

However most of the electrodes exhibit a relatively low capacitive current. Actually Kiran et al. reported capacitive current as low as 94 pA at a scan voltage of 200 mV s^{-1} , giving a double layer capacitance of 150 $\mu\text{F cm}^{-2}$ [154]. On electrode with 60 μm diameter, Hebert et al. found a double layer capacitance of 70 $\mu\text{F cm}^{-2}$ [155]. Chan et al. also report double layer capacitance values of 83 $\mu\text{F cm}^{-2}$ (deduced from impedance spectroscopy) [152]. Those values are 10–50 times above that of 4 $\mu\text{F cm}^{-2}$ usually obtained on diamond macro-electrodes [164]. These high values might be explained by a large amount of grain boundaries at the diamond surface, the relative roughness of as grown BNCD or to the high boron concentration inside the diamond film [164]. However even if those values are surprisingly high they are still far from the few mF cm^{-2} obtained for porous platinum, iridium oxide, Carbon nanotubes or PEDOT that are currently considered to be integrated in commercial devices. Those low background values compare to other electrodes are nevertheless interesting for in vivo neurotransmitter detection (see application of BDD diamond microelectrode).

Even if it possible to extract the double layer capacitance and an approximation of the charge injection limit of an electrode thanks to its potential window in a physiological medium, almost no paper gives both values. Finally only Hess et al. [159] used pulsed techniques to get the charge injection limit.

9.2.7.2 Impedance Spectroscopy on BNCD

Although a lot of papers reported on the EIS on BNCD probed with a redox couple for electrochemical sensing, few studies investigated the electrochemical impedance in PBS or salt medium. The impedance spectra on as grown BNCD MEA show high impedance modulus values when compared with the most efficient materials. Actually the reported values at 1 kHz are between 3 $\text{M}\Omega$ on 20 μm electrode in KCl electrode and 400 $\text{k}\Omega$ on a 60 μm electrode in PBS. We also

obtained using diamond values of 1 M Ω on 24 μ m electrodes in PBS. Such impedance modulus values mainly due to the relatively low double layer capacitance were observed using cyclic voltammetry. Only Chan et al. have reported an average impedance of 50 k Ω for a 30 μ m electrode in NaCl. These high impedances modulus are dramatic drawbacks for the viability of the micro-sized BNCD electrode for electrical neural interface application. That is why many other diamond technologies are under progress to overcome these issues. In the meantime, Gosso et al. and Pasquarelli et al. [137] showed that despite the rather low double layer capacitance and high impedance of diamond, it is possible to design electronics that allow sensing cardiac cells action potential.

9.2.8 *Diamond and MRI*

Given the increasing contribution of MRI for brain investigations, any microelectrode that is aimed at being implanted in the brain should not generate any image artefacts. This implies that no part of the device should have a magnetic susceptibility above that of water. In such a context, the compatibility of the heavily boron doped diamond with MRI studies was investigated. Actually carbon is a material presenting a magnetic susceptibility near to that of water. To assess the MRI compatibility, boron doped diamond films deposited on silicon substrates (3 \times 3 mm²) were implanted at the cortical surface of three rats [155]. The implants do not affect the MR signal and were extremely difficult to localize on all MR images, both at 2 and 6 months after implantation. At 2 months, a subcutaneous inflammatory reaction due to the surgery is visible on the structural images, but disappeared after 6 months. No major alteration of brain tissue due to the implant can be observed. B0 maps reveal an absence of significant field distortions due to the implant, since any B0 variations in the vicinity of the implants are much smaller than those observed at the base of the brain due to deoxy-hemoglobin in the internal jugular veins. This clearly indicates that boron doped diamond does not induce MRI artefacts.

9.2.9 *Application of Boron Doped Diamond Microelectrodes for Neural Interfacing*

The diamond devices were already used to sense or to stimulate the neural activity. In this section we give some example of application. A short example of the use of diamond as an electrochemical sensor for neurotransmitter detection is added in order to show the large application area of diamond in the neural interfacing.

9.2.9.1 *In vivo and in vivo Neurotransmitter Detection*

The ability to follow the dopamine release in the brain is a tremendous topic because dopamine is a key neurotransmitter involved in processes ranging from reward response to epilepsy. The biologists are thus looking for implantable and stable electrodes that can sense dopamine in vivo. Carbon fibers are currently the mostly used electrodes to meet the demand but cannot be used for long chronic studies. Diamond electrodes are very interesting for in vivo detection of neurotransmitters thanks to its low background current and its wide potential window. Its high biocompatibility and low fouling offers the possibility to measure in vivo during several weeks. Yoshimi et al. [165] thus managed to record in vivo the dopamine release for several weeks in the monkey and mouse striatum with diamond coated tungsten needle using fast scan cyclic voltammetry and amperometry technique. They were able to carry out a whole study on the phasic reward mechanism thanks to their diamond electrodes. Similarly Arumugam et al. showed that it is possible to sense in real-time in vivo dopamine release with diamond needles. They also get in vitro detection limit of 27 nM which is very near to that of carbon fiber sensors (11 nM) [165].

9.2.9.2 Direct Stimulation and Recording in vitro and in vivo

9.2.9.2.1 Recording and Stimulation in vitro on Organotypic Cultures

Halpern et al. showed the possibility to measure and to simulate the buccal motor neurons of the *Aplysia California* in vitro. They used a 30 μm BNCD electrode deposited at the top of a tungsten wire insulated with quartz [143]. Recording Cardiac Cells Culture Microelectrode arrays can be used in order to record the invoke activity of cell signals. For example, arrays of 64 pixel diamond microelectrodes have successfully been used by Maybeck et al., for the recording of the cardiomyocyte-like cell line HL-1 [166]. The study demonstrated that BNCD electrodes were able to detect cardiac cell action potentials as well as gold electrodes, while electrodes performed up to a factor of fourfold better than planar metal electrodes of the same diameter. BNCD electrodes survived the mechanical stresses of contractile cells without the defects commonly observed in other nanostructured materials after cell culture (loss of platinum black, removal of CNTs, tipping of pillars, D. Brüggemann unpublished results). This enabled to conclude that the diamond layer remained on the surface during cell contraction by the lack of thinning- induced defects after multiple cultures and the contractile tension generated in mature HL-1 cells (cells did not pull themselves off the surface), thus demonstrating that the diamond MEA's physical robustness makes it a durable and easy to handle device for repeated or long-term use, with promising interests for recording electrical signals from biological samples in addition to their established role in electrochemistry.

9.2.9.2.2 Recording the Cortex

As discussed previously, many breakthroughs in brain computer interface occurred during the last decade thanks to the development of outstanding microelectrode arrays. Nevertheless, highly stable materials, transparent for the body are still needed to get the ultimate material for neural interface. Chan et al. reported the first of all diamond devices implanted in the cortex [152]. They show that it is possible to perform acute in vivo recordings of action potential in the auditory cortex of the guinea pig. Even if the SNR was rather low ($\text{SNR} = 2$), this experiment is very promising for future investigation of all diamond devices. Actually once the SNR issue is overcome, such all diamond flexible devices might fulfill all the requirements for chronic implants.

9.2.9.2.3 Retina Stimulation

Recently, the concept of retinal prostheses was validated in clinical trials showing that such prostheses can enable blind patients to read short words, identify contrasted objects or follow lanes on the ground. These retinal prostheses aiming at restoring vision in patients having lost their photoreceptors are either placed in the subretinal space or on the epiretinal side in direct contact with either the outer or the inner limiting membrane both produced by glial Muller cells. In the first configuration, the subretinal implant will stimulate retinal bipolar cells, neurones normally postsynaptic to photoreceptors [167] whereas epiretinal implants are targeting retinal ganglion cells, spiking neurones sending visual information to the brain via their axon through the optic nerve. Although these implants have already restored some visual functions in patients, an increase in electrode resolution is required to further improve the restored visual performances to achieve face recognition, text reading or independent locomotion. Different 3D designs were already proposed to reach this objective using either pillars or wells on the implants.

9.2.10 *Advanced Diamond Electrodes for Neurophysiology*

As grown nanocrystalline diamond is a very promising material for neural interfacing thanks to its outstanding stability, biocompatibility properties and its MRI transparency. It is also a fantastic material for biosensing. This feature could be very interesting in the case of neurotransmitters sensing. However direct recording and stimulation are very difficult with diamond microelectrodes because of their high impedance and low double layer capacitance. A way to get rid of both those drawbacks is to increase the double layer capacitance. This could be achieved by changing the intrinsic material properties as proposed by Ganesan et al. [157] or by enlarging the active surface area for a given diameter by structuring the electrode surface. We discuss here this last option.

92.10.1 **Straightforward Structuration**

Many diamond structurations were developed to increase the diamond surface. In this context, nanowires were etched in the BNCD thanks to a metallic nanoparticle mask [168, 169]. The process consists in annealing a thin metallic layer deposited on the BNCD surface to obtain metallic nanoparticles that act as a mask during a plasma etching. The resulting wires have the same average diameter than the metallic nanoparticles. Smirnov et al. reported an increase of the active surface area by a factor 10. However such small diameter nanowires are too resistive because of their small section. This is an issue when it comes to impedance measurement. Larger pillars are nevertheless interesting and allow decreasing the impedance by a factor four. Considering that grown diamond impedance to be around 1 M Ω at 1 kHz, using such large pillars would reduce this value down to 200 k Ω . This would help enhancing the electrochemical performances.

Instead of using diamond wires, several teams suggested the use of diamond pores to avoid any problem linked to access resistance [170, 171]. They thus show that a local etching of the diamond surface is possible using metallic nanoparticles. The process starts exactly like the one used for the etching of diamond wires, with the annealing of a metallic layer. The diameter of the metallic nanoparticles defines the diameter of the pore. Then the sample is annealed at high temperature under a reductive atmosphere (generally a H₂ atmosphere) to etch the carbon through the metallic particles. This structure has not been tested yet for electrochemistry. Using 3D Scaffolds for BNCD Growth

92.10.1.1 Diamond Foam Using Nanospheres

More recently the use of 3D scaffolds for the growth of BNCD has been introduced. Kato et al. reported the coating compact silica 500 nm diameter spheres with BNCD [172]. They can tune the enlargement of the active surface area with number sphere layers. The surface was increased by 40 folds when 14 layers of sphere were used as a template for the BNCD growth.

92.10.1.2 Diamond Coated Carbon Nanotubes

We reported on the use of vertically carbon nanotubes as scaffolds the growth of BNCD [173]. Carbon nanotubes (CNTs) actually offer a large surface area and a high electrical conductivity to collect large currents, resulting in low interface impedances and large double layer capacitances. However they suffer from a lack of stability because of delamination and of small potential window. These issues may be overcome by strongly bonding the CNTs to the diamond substrate and coating them with diamond. By combining the CNT properties to the large potential window, high biocompatibility and stability of the BNCD obtained an all carbon material exhibiting almost all the

requirement for neural interfaces. The process consists in seeding the carbon nanotubes with a high density of diamond nanoparticles. This was accomplished thanks to a two-step electrostatic grafting process. Then the diamond nanoparticles are grown and coalesced thanks to a 450 °C plasma. The resulting material show a potential window of 2.7 V and double layer capacitance can be tuned by the length the carbon nanotubes, so as the interfacial impedance. For instance 3 µm long CNT coated with 30 nm BNCD allow decreasing the impedance by 100 fold and increasing the active surface area by 118 compare to BNCD electrode. Such amazing properties were also reported by May et al. [174].

9.2.11 Conclusion

Diamond is a unique material since it fulfils all the requirements for neural interfacing. Its biocompatibility was proven for many cells culture ranging from human bone marrow to rat neural cortex. More interesting, it is one of the rare conductive materials on which retinal ganglion cells can grow without using extracellular matrices proteins. It was also proven that glial cells cultures are reluctant to grow on diamond. These two results are very promising for the development of retinal prosthesis. However chronic study on diamond electrodes are still required to assess the complete absence of glial scars. In this context we are currently performing chronic in vivo impedance measurement with subretinal implants.

It is now possible to pattern diamond like silicon. This opens up the field of the implementation of high-density integrated diamond microelectrodes for high spatial resolution. Moreover, despite its rather high growth temperature, BNCD microelectrodes can be transferred on polymer flexible substrates to create very conformable and less invasive devices. Some new growth routes are under investigation to lower the diamond growth temperature for a direct growth a polymer substrate.

Diamond coated needles and diamond MEA already gave very nice results for in vivo dopamine and serotonin detection. They exhibited a long lifetime without fouling and very high sensitivity. Moreover some papers have already reported the direct recording and stimulation of action potential thanks to diamond microelectrodes.

The double layer capacitance and the charge injection limit of BNCD microelectrode are surprisingly high compare to that of macroelectrodes. This is very interesting for neural stimulation. Unfortunately, the current diamond microelectrodes seem to present a rather high impedance leading to high signal to noise ratio. In order to overcome these issues, new structured electrodes are developed to increase the surface area of the electrode. These technologies already showed a real improvement for both impedance and double layer capacitance. Within the next few months the current studies addressing in vitro and in vivo performances will soon state if such diamond electrode arrays are really as promising as expected.

References

1. JE. Graebner, S. Jin, GW. Kammlott, JA. Herb & CF. Gardinier, Large anisotropic thermal conductivity in synthetic diamond films, *Nature* 359, 401–403, 1992.
2. JPF. Sellschop 1979 *The Properties of Diamond* ed J E Field (New York: Academic).
3. P. Hess, The Mechanical properties of various chemical vapor deposition diamond structures compared to the ideal single crystal, *J Appl Phys*, 111 (5), 051101, 2012.
4. Yu. Borzdov, Yu. Pal'yanov, I. Kupriyanov, V. Gusev, A. Khokhryakov, A. Sokol, A. Efremov, HPHT synthesis of diamond with high nitrogen content from an Fe₃N–C system, *Diam and*

Relat Mater 11 (2002) 1863–1870.

5. FP. Bundy, HT. Hall, HM. Strong, RH. Wentorf Jr, Man-made Diamonds, *nature* 176, 51–55 (1955).
6. RF. Davis, JT. Glass, G. Lucovski, KJ. Bachman, Growth, characterization and device development in monocrystalline diamond films, Annual Report to Office of Naval research, 1987.
7. Q. Liang et al., Recent advances in high-growth rate single crystal CVD diamond, *Diam and Relat Mater*, 18, 5–8, pp 698–703 (2009).
8. JJ Gracio, QH Fan, JC Madaleno, Diamond growth by chemical vapour deposition. *J. Phys. D: Appl. Phys*, 43, 2010.
9. RS. Balmer et al., Chemical vapour deposition synthetic diamond: materials, technology and applications, *Journal of Physics: Condensed Matter* 21 (2009) 364221.
10. S. Koizumi, T. Teraji, H. Kanda, Phosphorus-doped chemical vapor deposition of diamond, *Diam and Relat Mater*, 9 (3–6); 935–940, 2000.
11. OA Williams, M. Nesldek, M. Daenen, S. Michaelson, A. Hoffman, E. Oswawa, Growth, electronic properties and application of nanodiamond, *Diam and Relat Mater*, 17 (7–10); 1080–1088 (2008).
12. R. Kalsih, Doping of Diamond, *Carbon*, 37 (5); 781–785, 1999.
13. E. Gheeraert, P. Gonon, A. Deneuville, L. Abello, G. Lucazeau, effect of boron incorporation on the quality of MPCVD diamond films, *Diam and Relat Mater*, 2 (5–7); 1993.
14. T. Klein, P. Achatz, J. Kacmarcik, C. Marcenat, J. Marcus, E. Bustarret et al. Metal-insulator transition and superconductivity in boron-doped diamond, *Phys Rev B*, 165313, 2007.
15. W. Adam, E. Berdermann, P. Bergonzo, W. De Boer, R. Bogani, E. Borchini et al. The development of diamond tracking detectors for the LHC, *Nuc. Inst. and Meth. in Phys. Res, Section A*, 514 (1–3); 79–86, 2003.
16. P. Bergonzo, A. Bambilla, D. Tromson, C. Mer, B. Guizard, RD. Marshall et al. CVD diamond for nuclear detections applications, *Nuc. Inst. and Meth. in Phys. Res, Section A*, 476 (3); 694–700, 2002.
17. P. Bergonzo, A. Brambilla, D. Tromson, C. Mer, C. Hordequin, B. Guizard et al. Diamond as a tool for synchrotron radiation monitoring: beam position, profile, and temporal distribution, *Diam. and Relat. Mater*, 9 (3–6); 960–964, 2000.
18. E. Vanhove et al., *Phys. Status Solidi*, vol. 204, no. 9, pp. 2931–2939, Sep. 2007.
19. A. Grill, *Diam. Relat. Mater.*, vol. 12, pp. 166–170, 2003.
20. L. Tang et al., *Biomaterials*, vol. 16, no. 6, pp. 483–8, Apr. 1995.
21. P. Ariano et al., *Diam. Relat. Mater.*, vol. 14, no. 3–7, pp. 669–674, Mar. 2005.
22. C. G. Specht et al., *Biomaterials*, vol. 25, no. 18, pp. 4073–8, Aug. 2004.
23. M. Amaral et al., *J. Nanomater.*, vol. 894352, 2008.
24. W. Okrój et al., *Diam. Relat. Mater.*, vol. 15, no. 10, pp. 1535–1539, Oct. 2006.
25. Y.-C. Chen et al., *Biomaterials*, vol. 30, no. 20, pp. 3428–35, Jul. 2009.
26. A. A. Rodrigues et al., *Diam. Relat. Mater.*, vol. 19, no. 10, pp. 1300–1306, Oct. 2010.
27. P. Bergonzo et al., *IRBM*, vol. 32, pp. 91–94, 2011.

28. T. Livache et al., *J. Pharm. Biomed. Anal.*, vol. 32, no. 4–5, pp. 687–696, Aug. 2003.
29. P. Sonthalia et al., *Anal. Chim. Acta*, vol. 522, no. 1, pp. 35–44, Sep. 2004. 30. B. Baur et al., *Langmuir*, vol. 24, no. 17, pp. 9898–9906, 2008.
31. A. Bongrain et al., *Langmuir*, vol. 27, no. 19, pp. 12226–34, Oct. 2011.
32. E. V. Jacques de sanoit, *Pat. PCT/EP2008/057032*, 2013.
33. R. G. C. M. E. Hyde, C.M. Welch, C.E. Banks, *Anal. Sci.*, vol. 21, no. 12, pp. 1421–1430, 2005.
34. M. C. Granger et al., *Anal. Chim. Acta*, vol. 397, no. 1–3, pp. 145–161, Oct. 1999.
35. M. Hupert et al., *Diam. Relat. Mater.*, vol. 12, pp. 1940–1949, 2003.
36. T. N. Rao et al., *J. Electrochem. Soc.*, vol. 148, no. 3, pp. 112–117, 2001.
37. C. Provent et al., *Electrochim. Acta*, vol. 49, no. 22–23, pp. 3737–3744, Sep. 2004.
38. A. Chatterjee et al., *Diam. Relat. Mater.*, vol. 11, no. 3–6, pp. 646–650, Mar. 2002.
39. J. S. Foord et al., *Phys. Chem. Chem. Phys.*, vol. 7, pp. 2787–2792, 2005.
40. M. Rievaj, *Sensors Actuators B. Chem.*, vol. 181, pp. 294–300, 2013.
41. M. Wei et al., *Microchim. Acta*, vol. 181, pp. 121–127, 2014.
42. L. Codognoto et al., *Diam. Relat. Mater.*, vol. 11, no. 9, pp. 1670–1675, Sep. 2002.
43. E. Fortin et al., *Bioelectrochemistry*, vol. 63, no. 1–2, pp. 303–6, Jun. 2004.
44. K. Kalcher, *Sensors Actuators B. Chem.*, vol. 194, pp. 332–342, 2014.
45. M. D. Koppang et al., *Anal. Biochem.*, vol. 71, no. 16, pp. 1188–1195, 1999.
46. J. de Sanoit et al., *Electrochim. Acta*, vol. 54, no. 24, pp. 5688–5693, Oct. 2009.
47. L. Svorc et al., *Diam. Relat. Mater.*, vol. 42, pp. 1–7, 2014.
48. B. V. Sarada et al., *Anal. Chem.*, vol. 72, no. 7, pp. 1632–1638, 2000.
49. M. Cristina et al., *Sensors Actuators B. Chem.*, vol. 188, pp. 263–270, 2013.
50. P. U. Arumugam et al., *Appl. Phys. Lett.*, vol. 102, p. 253107, 2013.
51. S. Siddiqui et al., *Biosens. Bioelectron.*, vol. 35, no. 1, pp. 284–290, 2012.
52. R. Andreozzi et al., *Catal. Letters*, vol. 53, pp. 51–59, 1999.
53. J. Iniesta et al., *Electrochim. Acta*, vol. 46, pp. 3573–3578, 2001.
54. M. A. Rodrigo et al., *J. Electrochem. Soc.*, vol. 148, no. 5, pp. 60–64, 2001.
55. P. Cañizares et al., *J. Electrochem. Soc.*, vol. 154, no. 11, pp. 165–171, 2007.
56. A. Kraft et al., *J. Hazard. Mater.*, vol. 103, no. 3, pp. 247–261, Oct. 2003.
57. B. Boye et al., *Electrochim. Acta*, vol. 51, no. 14, pp. 2872–2880, Mar. 2006.
58. A. Perret et al., *Diam. Relat. Mater.*, vol. 8, pp. 820–823, 1999.
59. C. Lévy-Clément et al., *Diam. Relat. Mater.*, vol. 12, no. 3–7, pp. 606–612, Mar. 2003.
60. T. Furuta et al., *Diam. Relat. Mater.*, vol. 13, pp. 2016–2019, 2004.
61. I. A. Cano et al., *Chem. Eng. J.*, vol. 211–212, pp. 463–469, 2012.
62. A. Cano et al., *Electrochem. commun.*, vol. 13, no. 11, pp. 1268–1270, 2011.
63. C. Agnès et al., *IOP Conf. Ser. Mater. Sci. Eng.*, vol. 16, p. 012001, Nov. 2010.

64. 4. W. Yang et al., *Nat. Mater.*, vol. 2, no. 1, pp. 253–258, 2003.
65. G.-J. Zhang et al., *Langmuir*, vol. 22, no. 8, pp. 3728–34, Apr. 2006.
66. N. Yang et al., *Angew. Chem. Int. Ed. Engl.*, vol. 47, no. 28, pp. 5183–5, Jan. 2008.
67. Y. Coffinier et al., *Langmuir*, vol. 23, no. 8, pp. 4494–7, Apr. 2007.
68. R. J. Hamers et al., *Diam. Relat. Mater.*, vol. 20, no. 5–6, pp. 733–742, May 2011.
69. A. D. Radadia et al., *Adv. Funct. Mater.*, vol. 21, pp. 1040–1050, 2011.
70. J. Wang et al., *Diam. Relat. Mater.*, vol. 15, no. 2–3, pp. 279–284, Feb. 2006.
71. P. Villalba et al., *Mater. Sci. Eng. C*, vol. 31, no. 5, pp. 1115–1120, Jul. 2011.
72. H. Olivia et al., *Electrochim. Acta*, vol. 49, no. 13, pp. 2069–2076, May 2004.
73. A. Härtl et al., *Nat. Mater.*, vol. 3, no. 10, pp. 736–42, Oct. 2004.
74. J. Rubio-Retama et al., *Langmuir*, vol. 22, no. 13, pp. 5837–42, Jun. 2006.
75. H. Kawarada, *Surf. Sci. Rep.*, vol. 26, no. 7, pp. 205–206, 1996
76. Y. Y. Un et al., *J. Appl. Phys.*, vol. 37, no. 11, pp. 1293–1296, 1998.
77. X. Gao et al., *J. Phys. Chem. C*, vol. 112, no. 7, pp. 2487–2491, Feb. 2008.
78. P. Strobel et al., *Nature*, vol. 430, pp. 242–244, 2004.
79. D. Pettrini et al., *J. Phys. Chem. C*, vol. 111, no. 37, pp. 13804–13812, Sep. 2007.
80. H. Kawarada et al., *Phys. Status Solidi*, vol. 208, no. 9, pp. 2005–2016, Sep. 2011.
81. D. Zhu et al., *Nat. Mater.*, vol. 12, no. 6, pp. 1–6, Jun. 2013.
82. H. Kawarada et al., *Phys. Status Solidi*, vol. 185, no. 1, pp. 79–83, May 2001.
83. K.-S. Song et al., *Jpn. J. Appl. Phys.*, vol. 43, no. No. 6B, pp. L814–L817, Jun. 2004.
84. K.-S. Song et al., *Phys. Rev. E*, vol. 74, no. 4, p. 041919, Oct. 2006.
85. S. Kuga et al., *J. Am. Chem. Soc.*, vol. 130, no. 40, pp. 13251–63, Oct. 2008.
86. A. R. Ruslinda et al., *Biosens. Bioelectron.*, vol. 40, no. 1, pp. 277–282, 2013.
87. O. Auciello et al., *IEE Microw. Mag.*, pp. 61–75, 2007.
88. A. Bongrain et al., *J. Micromechanics Microengineering*, vol. 19, p. 074015, 2009.
89. A. Bongrain et al., *Phys. Status Solidi*, vol. 2083, no. 9, pp. 2078–2083, 2010.
90. R. Manai et al., *Biosens. Bioelectron.*, vol. 60, pp. 311–317, 2014.
91. C. Blin et al., *Adv. Opt. Mater.*, vol. 1, pp. 963–970, 2013.
92. E. Chevallier et al., *Sensors Actuators B. Chem.*, vol. 154, no. 2, pp. 238–244, 2011.
93. E. Chevallier et al., *Sensors Actuators B. Chem.*, vol. 151, no. 1, pp. 191–197, 2010.
94. J. G. Rodríguez-madrid et al., *Sensors Actuators A. Phys.*, vol. 189, pp. 364–369, 2013.
95. V. Mortet, O. A. Williams, K. Haenen, *Phys. Status Solidi*, vol. 205, no. 5, pp. 1009–1020, 2008.
96. S. R. Pascal Mailley, Franck Omnes, Charles Agnes, Pat. PCT/FR2010/051399, 2010.
97. MB. Ahrens, JM. Li, MB. Orger, DN. Robson, AF. Schier, F. Engert et al. Brain-wide neuronal dynamics during motor adaptation in zebrafish, *Nature* 2012, 485; 471–477.
98. R. Homma, BJ Baker, L. Jin, O. Garaschuk, A. Konnerth, LB. Cohen, D. Zecevic, Widefield and two-photon imaging of brain activity with voltage- and calcium-sensitive dyes, *Phil. Trans. R. Soc. B* 2009.

99. Y. Le Chasseur, S. Dufour, G. Lavertu, C. Bories, M. Deschênes, R. Vallée, Y De Koninck, A microprobe for parallel optical and electrical recordings from single neurons in vivo, *Nature Methods* 2011, 8;319–325.
100. AR. Houwelin, M. Brech, Behavioural report of single neuron stimulation in somatosensory cortex, *Nature* 2007, 451; 65–68.
101. DJ. Bakkum, U. Frey, M. Radivojevic, TL. Russell, J. Müller, M. Fiscella, Tracking axonal action potential propagation on a high-density microelectrode array across hundreds of sites, *Nat. Comm.* 2013.
102. AL Benabid, P Pollak, C Gervason, and et al. Long-term suppression of tremor by chronic stimulation of the ventral intermediate thalamic nucleus. *Lancet*, 337:403–406, 1991.
103. MI. Hariz, P. Blomstedt, L. Zrinzo. 1947 Deep brain stimulation between 1947 and 1987: the untold story. *Neurosurgical Focus*, 29(2):E1, 2010.
104. MM. Lanotte, M. Rizzone, B. Bergamasco, and et al. Deep brain stimulation of the subthalamic nucleus: anatomical, neurophysiological, and outcome correlations with the effects of stimulation. *J Neurol Neurosurg Psychiatry*, 72:53–58, 2002.
105. ED. Keefer, Barry R. Botterman, Mario I. Romero, Andrew F. Rossi, and Guenter W. Gross. Carbon nanotube coating improves neuronal recordings. *Acta Neurochir Suppl*, 106:337–341, 2010.
106. R. van den Brand, J. Heutschi, Quentin Barraud, J. DiGiovanna, K. Bartholdi, M. Huerlimann et al. Restoring voluntary control of locomotion after paralyzing spinal cord injury. *Science*, 336:1182–1185, 2012.
107. N. Dominici, U. Keller, H. Vallery, L. Friedli, and R. Van Den Brand et al. Versatile robotic interface to evaluate, enable and train locomotion and balance after neuromotor disorders. *Nature Medecine*, 2012.
108. M Heim, L Rousseau, S Reculosa, V Urbanova, C Mazzocco, S Joucla et al. Combined macro-mesoporous microelectrode arrays for low-noise extracellular recording of neural networks, *J Neurophysiol* 108:1793–1803, 2012.
109. NA. Kotov, J.O. Winter, IP. Clements, E. Jan, BP. Timko, S. Campidelli, *Nanomaterials for Neural Interfaces*, *Adv. Mater* 2009, 21, 1–35.
110. G. Baranauskas, E. Maggiolini, E. Castagnola, A. Ansaldo, A. Mazzoni, G. N. Angtozi, and A. Vato et al. Carbon nanotube composite coating of neural microelectrodes preferentially improves the multiunit signal to noise ratio. *J. Neural Eng*, 8, 2011.
111. V. Lovat, D. Pantarotto, L. Lagostena, B. Cacciari, M. Grandolfo, and M. Righi et al. Carbon nanotube substrates boost neuronal electrical signaling. *Nano letters*, 5(6):1107–1110, 2005.
112. S. Venkatraman, J. Hendricks, Z. A. King, AJ. Sereno, S. Richardson-Burns, D. Martin, JM. Carmena, *In Vitro and In Vivo Evaluation of PEDOT Microelectrodes for Neural Stimulation and Recording*, *IEEE Transactions On Neural Systems And Rehabilitation Engineering*, 2011, 19(3); 307–315.
113. Seth J. Wilks, SM. Richardson-Burns, JL. Hendricks, DC. Martin, KJ. Otto, Poly(3,4-ethylenedioxythiophene) as a micro-neural interface material for electrostimulation, *Frontiers in neuroengineering* 2009, 2.
114. SF. Cogan, J. Ehrlich, TD. Plante, A. Smirnov, Do. B Shire, M. Gingerich, JF. Rizzo, Sputtered iridium oxide films for neural stimulation electrodes, *Jour. Biomed. Mater. Res Part B* 2009, 89(2);353–361.
115. S. Gawad, M. Giugliano, M. Heuschkel, B. Wessling, H. Markram, U. Schnakenberg et al.

- Substrate arrays of iridium oxide microelectrodes for in vitro neuronal interfacing, *frontiers in neural engineering* 2009, 2.
116. G. Lind, CE. Linsmeier, J Schouenborg, The density difference between tissue and neural probes is a key factor for glial scarring. *Sci. Rep.* 3, 2942.
 117. VS. Polikov, PA. Tresco, WM. Reichert, Response of brain tissue to chronically implanted neural electrodes, *Journal of Neuroscience Methods* 148 (2005) 1–18.
 118. Y. Zhong and RV Bellamkonda, Biomaterials for the central nervous system, *J. R. Soc. Interface* (2008) 5, 957–975.
 119. SF. Cogan, AA. Guzeliam, WF. Agnew, Ted G. H. Yuen Douglas B. McCreery, Over-pulsing degrades activated iridium oxide films used for intracortical neural stimulation, *Journal of Neuroscience Methods* 137 (2004); 141–150.
 120. Lilach Bareket-Keren and Yael Hanein, Carbon nanotube-based multi electrode arrays for neuronal interfacing: progress and prospects, *frontiers in neural circuit*, 2012, 6.
 121. RW. Griffith, DR. Humphrey, Long-term gliosis around chronically implanted platinum electrodes in the Rhesus macaque motor cortex, *Neurosci Lett.* 2006;406(1–2):81–6.
 122. ES. Ereifej, S. Khan, G. Newaz, J. Zhang, GW. Auner, PJ. VandeVord, Comparative assessment of iridium oxide and platinum alloy wires using an in vitro glial scar assay, *Biomed Microdevices* 2013, 15:917–924.
 123. S. Chen and MG. Allen, Extracellular matrix-based materials for neural interfacing, *MRS Bulletin* 2012, 37, 606–613.
 124. A. Mazzatenta, M. Giugliano, S. Campidelli, L. Gambazzi, L. Businaro, H. Makram et al. Interfacing neurons with carbon nanotubes: Electrical signal transfer and synaptic stimulation in cultured brain circuits. *The Journal of Neuroscience*, 27:6931–6936, 2007.
 125. CA Poland, R Duffin, I Kinloch, A Maynard, WAH Wallace et al. Carbon nanotubes introduced into the abdominal cavity of mice showasbestos-like pathogenicity in a pilot study. *Nature Nanotechnology*, 3:423–428, 2008.
 126. LT Hall. et al. High spatial and temporal resolution wide-field imaging of neuron activity using quantum NV-diamond. *Sci. Rep.* 2, 401, 2012.
 127. G. Buzsáki, CA. Anastassiou and C. Koch The origin of extracellular fields and currents EEG, ECoG, LFP and spikes, *Nature Review Neuroscience*, 3, 407–20, 2012.
 128. MM. Heinricher, Principles of extracellular single unit recodring in Microelectrode recording in movement disorder surgery Zvi Israel, Kim J. Burchiel—New York 2011.
 129. T. Schwartz, The thermodynamic functions of membrane physiology. In *Biophysics and Physiology of Excitable Membrane*. W. J. Adelman, Jr., editor. Van Nostrand Reinhold Co., New York. 47–95, 1971.
 130. DC. Chang, Dependence of cellular potential on ionic concentrations, *Biophysical journal*, 43; 149–156, 1983.
 131. N. Joye, A. Schmid, Y. Leblebici, Electrical modeling of the cell–electrode interface for recording neural activity from high-density microelectrode arrays, *Neurocomputing*, 73;250– 9, 2009.
 132. V. Thakore, P. Molnar, and JJ. Hickman, An Optimization-Based Study of Equivalent Circuit Models for Representing Recordings at the Neuron–Electrode Interface; *Transactions on biomedical engineering*, 59, (8), 2012.
 133. S.F. Cogan, Neural Stimulation and Recording electrodes, *Annu. Rev. Biomed. Eng.* 10;275–

309; 2008.

134. MLAV. Heien, MA. Johnson, and RM. Wightman, Resolving Neurotransmitters Detected by Fast-Scan Cyclic Voltammetry, *Analytical chemistry*, 76; 5697–5704, 2004.
135. H.W Ott, *Noise Reduction techniques in electronic systems*, 2nd Edition ed. New York: Wiley and Sons, pp 251.
136. J. Neuburger, T. Lenarz, A. Lesinski-Schiedat, A. Buchner Spontaneous increases in impedance following cochlear implantation: suspected causes and management *Int J Audiol*, 48 (5) (2009), pp. 233–239.
137. S. Gosso, A. Marcantoni, M. Turturici, A. Pasquarelli, E. Carbone, V. Carabelli. Multipurpose nanocrystalline boron-doped diamond MEAs for amperometric, potentiometric and pH recordings from excitable cells MEA meeting proceedings, 323–324, 2012.
138. V. Paget, J. A. Sergent, R. Grall, S. Altmeyer-Morel, H. A. Girard, T. Petit, C. Gesset, M. Mermoux, P. Bergonzo, J. C. Arnault, and S. Chevillard, Carboxylated nanodiamonds are neither cytotoxic nor genotoxic on liver, kidney, intestine and lung human cell lines, *Nanotoxicology*, 2013.
139. E. Perevedentseva, YC. Lin, M. Jani, CL. Cheng Biomedical applications of nanodiamonds in imaging and therapy *Nanomedicine* (2013) 8(12), 2041–2060.
140. A. Thalhammer, RJ. Edgington, LA. Cingolani, R. Schoepfer, RB. Jackman, The use of nanodiamond monolayer coatings to promote the formation of functional neuronal networks, *Biomaterials* 31; 2097–2104, 2010.
141. P.W. May, E.M. Regan, A. Taylor, J. Uney, A.D. Dick, J. McGeehan, Spatially controlling neuronal adhesion on CVD diamond, *Diam and Relat Mater* 23; 100–104, 2012.
142. A. Bendali, C. Agnès, S. Meffert, V. Forster, A. Bongrain, JC. Arnault, JA. Sahel, A. Offenhäusser, P. Bergonzo, S. Picaud, Distinctive Glial and Neuronal Interfacing on Nanocrystalline Diamond, *Plos One*, 9(3); e92562, 2014.
143. JM. Halpern, S. Xie, GP. Sutton, BT. Higashikubo, CA. Chestek, H. Lu, et al. Martin, Diamond electrodes for neurodynamic studies in *Aplysia californica*, *Diam and Relat Mater* 2006, 15; 183–187.
144. J. Park, JJ. Galligan, GD. Fink, and GM. Swain, In Vitro Continuous Amperometry with a Diamond Microelectrode Coupled with Video Microscopy for Simultaneously Monitoring Endogenous Norepinephrine and Its Effect on the Contractile Response of a Rat Mesenteric Artery, *Anal. Chem.* 2006, 78, 6756–6764.
145. A. Suzuki, TA. Ivandini, K. Yoshimi, A. Fujishima, G. Oyama, T. Nakazato et al. Fabrication, Characterization, and Application of Boron-Doped Diamond Microelectrodes for in Vivo Dopamine Detection, *Anal. Chem.*, 2007, 79, 8608–8615.
146. M. Pagels, CE. Hall, NS. Lawrence, A Meredith, TG. J. Jones et al. All-Diamond Microelectrode Array Device, *Anal. Chem*, 77, 3705–3708, 2005.
147. K Peckova, J Berek Boron Doped Diamond Microelectrodes and Microelectrode Arrays in Organic Electrochemistry *Curr. Org. electrochem.* 15(17); 3014–3028, 2011.
148. V. Carabelli, S. Gosso, A. Marcantoni, Y. Xu, E. Colombo, Z. Gao, E. Vittone, E. Kohn, A. Pasquarelli, E. Carbone, Nanocrystalline diamond microelectrode arrays fabricated on sapphire technology for high-time resolution of quantal catecholamine secretion from chromaffin cells, *Biosensors and Bioelectronics* 26; 92–98, 2010.
149. KL. Soh, WP. Kang, JL. Davidson, S. Basu, YM. Wong, DE. Cliffl, AB. Bonds, GM. Swain, Diamond-derived microelectrodes array for electrochemical analysis, *Diam and Relat Mater*,

13;2009–2015, 2004.

150. W. Smirnov, N. Yang, R. Hoffmann, J. Hees, H. Obloh, W. Muller-Sebert, and CE. Nebel, Integrated All-Diamond Ultramicroelectrode Arrays: Optimization of Faradaic and Capacitive Currents, *Anal. Chem*, 83;7438–7443.
151. Kiran R, Scorsone E, Mailley P, Bergonzo P, Quasi-real time quantification of uric acid in urine using boron doped diamond microelectrode with in situ cleaning, *Anal. Chem*, 84; 10207–10213, 2012.
152. HY. Chan, DM. Aslam, JA. Wiler, B. Casey, A Novel Diamond Microprobe for NeuroChemical and -Electrical Recording in Neural Prosthesis, *JMEMS*, 18(3); 511–521, 2009.
153. MW. Varney, DM. Aslam, A. Janoudi, HY. Chan, DH. Wang, Polycrystalline-Diamond MEMS Biosensors Including Neural Microelectrode-Arrays, *Biosensors*, 1; 118–133, 2011.
154. R. Kiran, L. Rousseau, G. Lissorgues, E. Scorsone, A. Bongraink, B. Yvert, Serge Picaud, Pascal Mailley and Philippe Bergonzo, Multichannel Boron Doped Nanocrystalline Diamond Ultramicroelectrode Arrays: Design, Fabrication and Characterization, *Sensors*, 12; 7669–7681, 2012.
155. C. Hébert, J. Warnking, A. Depaulis, D. Eon, P. Mailley, F. Omnes, Microfabrication characterization and in vivo MRI compatibility of all diamond microelectrode array for neural interfacing, submitted to *Material Science and engineering:C*.
156. C. Hébert, E. Scorsone, A. Bendali, R. Kiran, M. Cottance, H.A. Girard, J. Degardin, E. Dubus, G. Lissorgues, L. Rousseau, S. Picaud, P. Bergonzo, Boron doped Diamond Biotechnology: from sensors to neurointerfaces, *Faraday discussion* 172, 2014.
157. K. Ganesan, DJ. Garrett, A. Ahnood, MN. Shivdasani, W. Tong, AM. Turnley et al. An all-diamond, hermetic electrical feedthrough array for a retinal prosthesis, *Biomaterials* 35;908–915, 2014.
158. P. Bergonzo, A. Bongrain, E. Scorsone, A. Bendali, L. Rousseau, and G. Lissorgues et al. Diamond-on-polymer microelectrode arrays fabricated using a chemical release transfer process. *Micromechanical Systems*, 20(4):867–875, 2011.
159. AE. Hess, DM. Sabens, HB. Martin, and CA. Zorman, Diamond-on-Polymer Microelectrode Arrays Fabricated Using a Chemical Release Transfer Process, *JMEMS*, 20(4), 867– 875, 2011.
160. Scorsone, E.; Saada, S.; Arnault, J. C.; Bergonzo, P. *Journal of Applied Physics* 2009, 106, 014908.
161. DH. Kim, J. Viventi et al. Dissolvable films of silk fibroin for ultrathin conformal biointegrated electronics, *Nature material* 2010, 9; 511–517.
162. Sommerhalder J, Rappaz B, de Haller R, Fornos AP, Safran AB and Pelizzone M, *Vision Res* 2004, 44, 1693–1706.
163. Djilas M, Oles C, Lorach H, Bendali A, Degardin J, Dubus E et al. Three-dimensional electrode arrays for retinal prostheses: modeling, geometry optimization and experimental validation. *J Neural Eng* 2011, 8, 046020.
164. T. Watanabe, TK. Shimizu, Y. Tateyama, Y. Kim, M. Kawai, Y. Einaga, Giant electric double-layer capacitance of heavily boron-doped diamond electrode.
165. Kenji Yoshimi, Yuuki Naya, Naoko Mitani, Taisuke Kato, Masato Inoue, Shihoko Natori, et al Phasic reward responses in the monkey striatum as detected by voltammetry with diamond microelectrodes, *Neuroscience Research* 71 (2011) 49–62.

166. Maybeck V, Edgington R, Bongrain A, Welch JO, Scorsone E, Bergonzo P, Jackman RB, Offenhäusser A., Boron-doped nanocrystalline diamond microelectrode arrays monitor cardiac action potentials. *Adv Healthc Mater.* 2014 Feb;3(2):283–9.
167. Zrenner E, Bartz-Schmidt KU, Benav H, Besch D, Bruckmann A et al Subretinal electronic chips allow blind patients to read letters and combine them to words. *Proc Biol Sci*, 2011, 278, 1489–1497.
168. Janssen W, Faby S, Gheeraert E. Bottom-up fabrication of diamond nanowires arrays. *Diam Relat Mater* 2011; 20(5–6): 779–81.
169. Smirnov W, Kriele A, Yang N, Nebel CE. Aligned diamond nanowires: Fabrication and characterization for advanced applications in bio-and electrochemistry. *Diam Relat Mater* 2010; 19(2–3): 186–9.
170. Mehedi HA, Arnault JC, Eon D, Hébert C, Carole D, Omnes F et al. Etching mechanism of diamond by Ni nanoparticles for fabrication of nanopores. *Carbon* 2013; 59; 448–56.
171. Smirnov W, Hess JJ, Brink D, Sebert WM, Kriele A, and Williams OA et al. Anisotropic etching of diamond by molten ni particles. *Appl Phys Lett*, 2010.
172. Kato H, Hess J, Hoffmann R, Wolfer M, Yang N, Yamasaki S et al. Diamond foam electrodes for electrochemical applications. *Electrochem Com* 2013; 33; 88–91.
173. Hébert C., Mazellier J-P., Scorsone E., Mermoux M., Bergonzo P. Boosting the electrochemical properties of diamond using a vertically aligned CNT scaffold, *Carbon* 2014, 71, 27–33.
174. H. Zanin, PW May, DJ. Firmin, D. Plana, SM. Viera, WI Milne, EJ Corat, *ACS Appl Mater Interfaces.* 2014 22;6(2):990–5.